Available online at www.sciencedirect.com

ScienceDirect

Geochimica et Cosmochimica Acta 261 (2019) 191–209

Geochimica et Cosmochimica Acta

www.elsevier.com/locate/gca

Multiple negative molybdenum isotope excursions in the Doushantuo Formation (South China) fingerprint complex redox-related processes in the Ediacaran Nanhua Basin

Chadlin M. Ostrander [a,*], Swapan K. Sahoo [b,c], Brian Kendall [d], Ganqing Jiang [b], Noah J. Planavsky [e], Timothy W. Lyons [f], Sune G. Nielsen [g], Jeremy D. Owens [h], Gwyneth W. Gordon [a], Stephen J. Romaniello [a], Ariel D. Anbar [a,i]

[a] School of Earth and Space Exploration, Arizona State University, Tempe, AZ, USA
[b] Department of Geoscience, University of Nevada, Las Vegas, NV, USA
[c] Equinor US, Houston, TX, USA
[d] Department of Earth and Environmental Sciences, University of Waterloo, Waterloo, Ontario, Canada
[e] Department of Geology and Geophysics, Yale University, New Haven, CT, USA
[f] Department of Earth Sciences, University of California, Riverside, CA, USA
[g] Department of Geology and Geophysics, Woods Hole Oceanographic Institution, Woods Hole, MA, USA
[h] Department of Earth, Ocean, and Atmospheric Science, National High Magnetic Field Laboratory, Florida State University, Tallahassee, FL, USA
[i] School of Molecular Sciences, Arizona State University, Tempe, AZ, USA

Received 31 January 2019; accepted in revised form 8 July 2019; Available online 16 July 2019

Abstract

The Ediacaran Doushantuo Formation offers one of the most complete and extensively studied records of end-Neoproterozoic biotic and environmental change. Here, we report multiple coeval negative molybdenum (Mo) isotope excursions (to as low as $\delta^{98}Mo_{NIST+0.25} = -2.24 \pm 0.10‰$; 2SD) in shales from four separate sites in South China (Rongxi, Taoying, Wuhe, and Yuanjia) that preserve the Doushantuo Formation. The negative δ^{98}Mo excursions appear coincident with previously discovered and seemingly peculiar redox-sensitive element (RSE) patterns in the same sedimentary rocks. We propose that these geochemical trends can be explained by some combination of (a) enhanced local marine oxygenation in the sedimentary basin where the Doushantuo Formation was originally deposited (the Nanhua Basin) and (b) changes in the degree of connectivity between this paleo basin and the open ocean. Enhanced local marine oxygenation, by exposing more sediments in the Nanhua basin to H_2S-poor conditions, could have hindered quantitative tetrathiomolybdate formation within these sediments. Local marine oxygenation could have also stimulated the operation of a Mn oxide shuttle. Today, both of these processes are shown to promote the retention of lighter-mass Mo isotopes in sediments and also govern RSE enrichment patterns. Alternatively, or in addition, the Nanhua Basin may not have maintained an uninterrupted connection with the open ocean during the entirety of the Ediacaran Period. The negative δ^{98}Mo excursions occur coincident with sea level highstands that could have also exposed more sediments in the basin to H_2S poor conditions and/or catalyzed the operation of a local Mn oxide shuttle. When trying to infer temporal changes in ancient global ocean redox, it is important to consider the influence of sea level changes and associated variations in local depositional conditions on stratigraphic trends in RSE enrichments and isotope compositions.

* Corresponding author.
E-mail address: cmostran@asu.edu (C.M. Ostrander).

https://doi.org/10.1016/j.gca.2019.07.016
0016-7037/

1. INTRODUCTION

The tempo of marine oxygenation during the Ediacaran Period (635–542 million years ago, or Ma) is debated. It is generally accepted that the shallow ocean was oxygenated throughout the Ediacaran (Lowenstein et al., 2013, and references therein). However, two predominant viewpoints exist for the O_2 contents of the deeper waters: (1) always anoxic (Johnston et al., 2013; Sperling et al., 2015) or (2) subject to episodic ocean oxygenation events (OOEs [Fike et al., 2006; McFadden et al., 2008; Kendall et al., 2015; Sahoo et al., 2012, 2016]). Resolution of this debate is important to understanding what role – if any – O_2 levels in Ediacaran oceans played in controlling the dynamics of early animal evolution (Knoll, 2011; Lenton et al., 2014).

The most commonly invoked evidence for Ediacaran OOEs comes in the form of redox-sensitive element (RSE; e.g., V, Mo, Re, and U) enrichments in shales – foremost from the Doushantuo Formation of South China (Sahoo et al., 2012, 2016). In the modern ocean, widespread oxygenation supports large seawater reservoirs of RSE, which enables strong sedimentary RSE accumulation in the anoxic organic-rich marine sediments that cover a small percentage of the ocean floor (e.g., Scott et al., 2008; Sahoo et al., 2012; Partin et al., 2013; Sheen et al., 2018). Intuitively, ancient black shales deposited in the primarily anoxic Precambrian global ocean (Reinhard et al., 2013) and also during episodes of extensive global ocean anoxia during the Cambrian (Gill et al., 2011; Owens et al., 2016) have much lower RSE abundances because widespread burial in anoxic sediments depleted RSE seawater reservoirs. The transition away from a predominantly anoxic Precambrian ocean and toward a well-oxygenated one more similar to today's is expected to have led to first-order increases in RSE seawater reservoirs and sedimentary RSE accumulation. The geochemical fingerprints of at least the initial, likely transient phases of this transition seem to have been captured in black shales from the Ediacaran Doushantuo Formation (Scott et al., 2008; Sahoo et al., 2012, 2016).

Some RSE trends in the Doushantuo Formation are peculiar, causing some researchers to question their straightforward link to Ediacaran ocean oxygenation (e.g., Miller et al., 2017). For example, some RSEs are enriched in Doushantuo shales to levels comparable to those found in only the most RSE-enriched Phanerozoic shales (V in particular, which reaches wt. % abundances [Sahoo et al., 2016]). Furthermore, during the ca. 580 Ma OOE recorded in Doushantuo shales, some RSEs are not enriched at all (e.g., Mo [Sahoo et al., 2016], although pyrite from these shales is enriched in Mo [Gregory et al., 2017]). Lastly, the widespread ocean oxygenation implied by the episodes of RSE enrichment in the Doushantuo Formation does not seem to be supported by some geochemical compilations (e.g., a recent compilation of the Fe speciation record [Sperling et al., 2015]).

Using the Mo isotope paleoredox proxy, we provide new perspective on the sedimentary RSE record from South China. The Mo isotope composition of organic-rich marine shales can be an effective way to track redox changes in Earth's ancient oceans (see a recent review by Kendall et al., 2017). For example, sedimentary rocks deposited under anoxic and sulfidic (hereafter referred to as euxinic) conditions in restricted basins can sometimes capture the coeval seawater δ^{98}Mo (e.g., in deep portions of the Black Sea [Neubert et al., 2008], Kyllaren fjord [Noordmann et al., 2015], and Lake Rogoznica [Bura-Nakić et al., 2018]). Transfer of the seawater δ^{98}Mo to marine sediments is possible in these settings because nearly all Mo in marine bottom waters can be transferred to underlying sediments. The Mo isotope composition of seawater is a useful parameter because it is thought to be a direct consequence of the relative distribution of oxic versus euxinic conditions on the seafloor (Barling et al., 2001; Arnold et al., 2004). For these reasons, the primary application of the Mo isotope paleoredox proxy to date has been as a tool for estimating global marine redox conditions using ancient sedimentary rocks originally deposited under euxinic conditions (Kendall et al., 2017).

In the majority of modern marine settings, however, including some that are defined as euxinic, near-quantitative transfer of Mo from deep water to sediments *does not* occur and results in sedimentary δ^{98}Mo that are isotopically lighter than the coeval seawater value (e.g., Arnold et al., 2004; Poulson et al., 2006; Poulson-Brucker et al., 2009; Nägler et al., 2011; Noordmann et al., 2015). In these settings, incomplete transfer of Mo from seawater to sediments and the complexation of Mo with Fe oxide minerals (Goldberg et al., 2009, 2012), Mn oxide minerals (Wasylenki et al., 2008), and organic matter (King et al., 2018) – as well as the persistence of intermediate thiomolybdate species (Neubert et al., 2008) – results in the preferential retention of lighter-mass Mo isotopes in these sediments. Therefore, a case can be made that an important utility of the Mo isotope paleoproxy rests with tracking these processes – rather than, or in addition to, its value as a proxy tracking global seawater δ^{98}Mo.

We have measured the Mo isotope compositions of the same shale samples from the Doushantuo Formation from South China that yielded the RSE evidence for OOEs (i.e., those analyzed in Sahoo et al., 2012, 2016). Redox-sensitive elements, in addition to their sensitivity to global marine redox conditions, are also sensitive to the complexation processes that affect sedimentary δ^{98}Mo (e.g., Morford et al., 1999, 2005; Tribovillard et al., 2006; Scholz et al., 2011, 2013, 2018). Therefore, by identifying these complexation processes using Mo isotopes, we can assess their possible contribution to the RSE patterns in the Doushantuo Formation.

2. MATERIALS AND METHODS

2.1. The Doushantuo Formation from South China

We targeted shales of the Ediacaran Doushantuo Formation (~635–560 Ma [Condon et al., 2005; An et al., 2015]) in multiple sections from the Yangtze platform in South China, a paleo-location referred to as the Nanhua Basin (Jiang et al., 2011) (Fig. 1). In order of increasing distance from the paleo-shoreline, we measured Mo

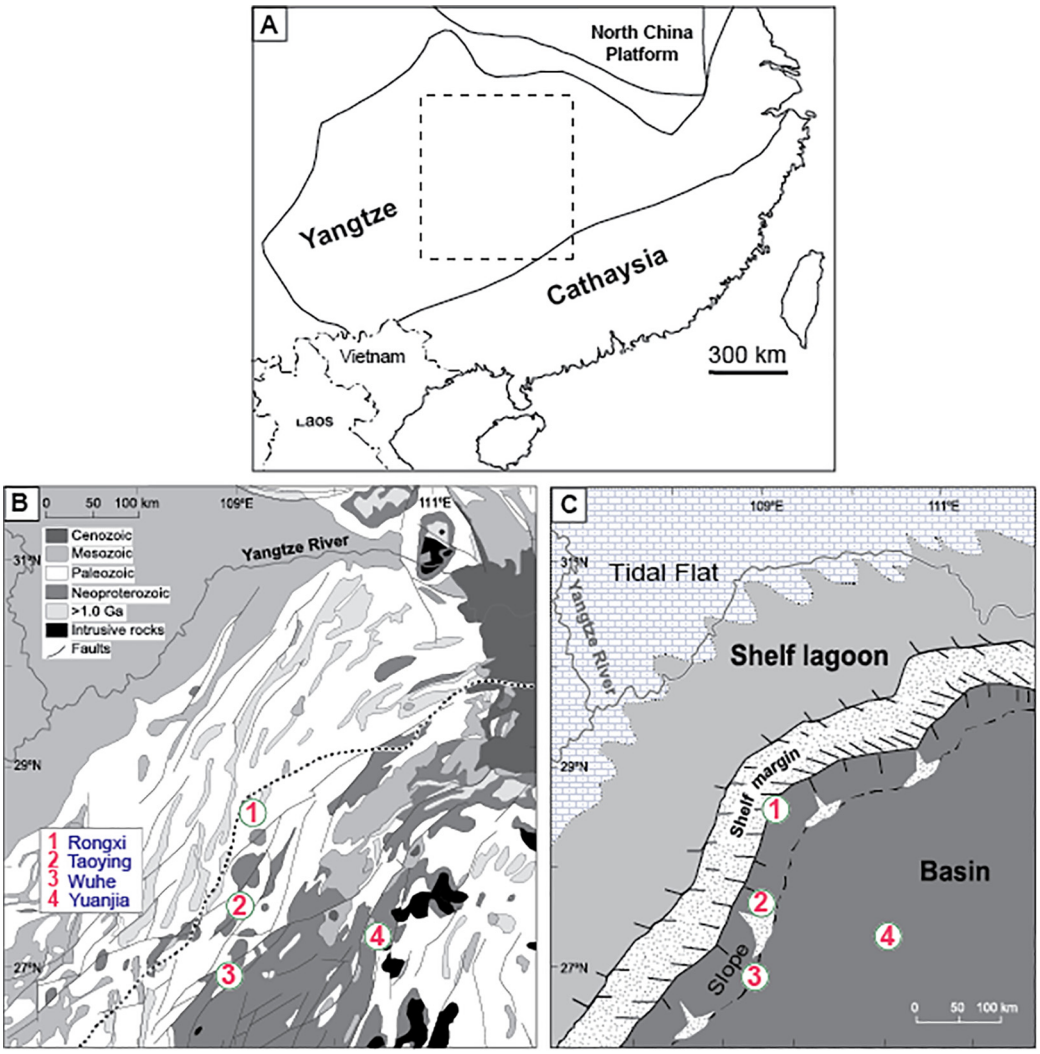

Fig. 1. Tectonic, geological, and paleogeographic maps for the Yangtze platform of South China. (a) Tectonic map showing the Yangtze and Cathaysia blocks in China, with the dashed rectangle corresponding to the area depicted in B and C. (b) Simplified geological map showing exposures of strata in the central Yangtze platform of South China. The dotted line signifies the position of the platform margin during the late Neoproterozoic, and each number represents a site from which shales used in this study were originally collected. (c) Paleogeographic reconstruction of the Nanhua Basin during the Ediacaran Period. Figures modified from Jiang et al. (2011). (For interpretation of the references to color in this figure legend, the reader is referred to the web version of this article.)

isotope compositions of shales originally deposited on the continental slope of the Nanhua Basin from sites at Rongxi, Taoying, and Wuhe and of shales deposited deeper within the basin from the Yuanjia site. A case has been made previously that sedimentary rocks deposited in the slope and basin environments of the Nanhua Basin were connected with the open ocean during deposition of the Doushantuo Formation (Jiang et al., 2011; Sahoo et al., 2012).

We targeted shales from the entire Wuhe site (Members II through IV) and shales deposited during the purported OOEs from lowermost Member II (Rongxi, Taoying, and Yuanji), Member III (Taoying), and Member IV (Rongxi, Taoying) of the other sections (Fig. 2). All of these sections are described in detail in previous work (Jiang et al., 2011; Sahoo et al., 2012, 2016); only a very brief overview is provided here.

Much effort has been dedicated to stratigraphically correlating the many sections from South China that preserve the Doushantuo shales. For ease of correlation, the Doushantuo Formation is split into four distinct members based primarily on lithology (Fig. 2). The cap carbonates overlying the glacial diamictites of the Marinoan glaciation are assigned to Member I (635.2 ± 0.6 Ma [Condon et al., 2005]). Cap carbonates of Member I are overlain by mixed carbonate-siliciclastics, with the onset of Member II in slope sections typically signified by a transition to shale-dominated units. In the shelf and upper slope sections, including the Rongxi section, Member III is dominated by carbonates, but equivalent strata in the lower slope and basin sections are shale-dominated, with carbonate beds unevenly distributed in the lower and upper parts. Black shales of Member IV are widespread across the entire Nanhua Basin and are seen in all measured sections.

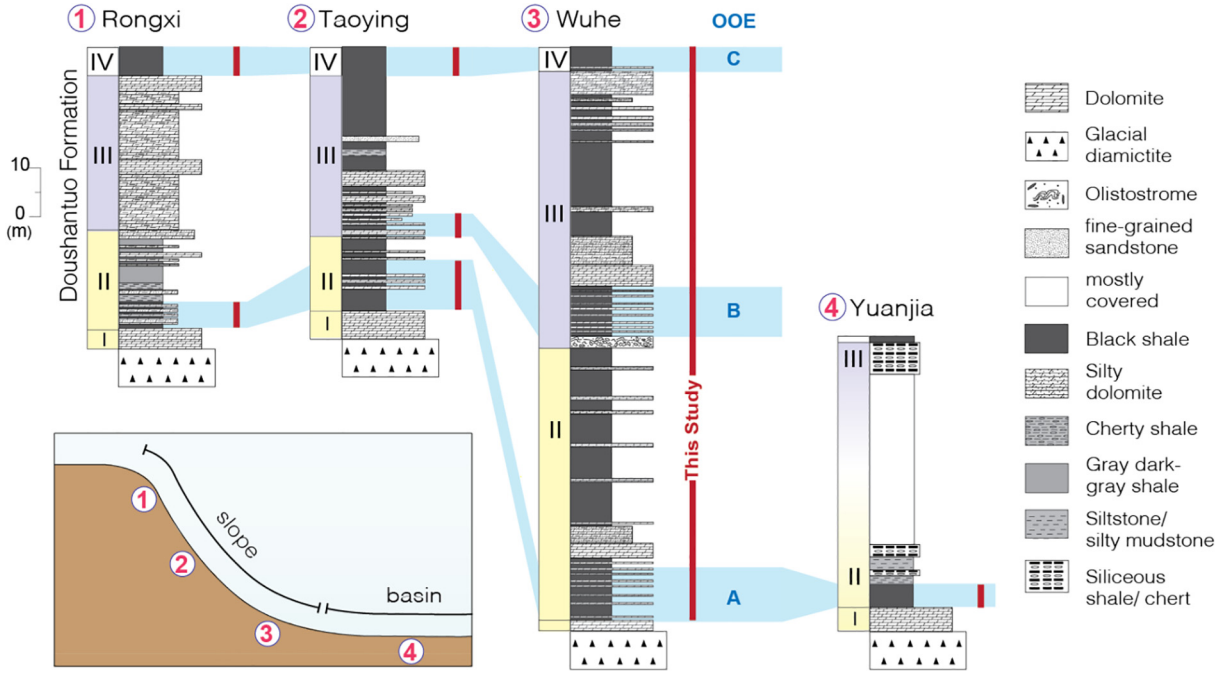

Fig. 2. Sections analyzed in this study. For a detailed description of lithology, see Jiang et al. (2011) and Sahoo et al. (2012). Section intervals targeted here are signified by the vertical red bar. Previously identified Ediacaran ocean oxygenation events (OOEs) are identified by blue boxes (A, B, and C [Sahoo et al., 2011, 2016]). Stratigraphic columns, slope reconstruction, and legend are modified from Jiang et al. (2011) and Sahoo et al. (2016). (For interpretation of the references to color in this figure legend, the reader is referred to the web version of this article.)

2.2. Mo isotope methods

All sample digestion, chromatography, and instrumental analysis was completed at the W. M. Keck Foundation Laboratory for Environmental Biogeochemistry at Arizona State University. Whole-rock powders were ashed and digested and concentrations were analyzed via quadrupole Inductively Coupled Plasma Mass Spectrometry (ICPMS) using techniques outlined in previous work (Olson et al., 2019). Subsequently, enough sample was taken from each digested stock solution to provide 125 ng of Mo, and thereafter spiked with an optimal amount of calibrated synthetic Mo isotope double spike (^{97}Mo and ^{100}Mo) to correct for isotopic fractionation during chromatography and for instrumental mass bias (Siebert et al., 2001). Molybdenum purification involved the typical two-step anion and cation column procedure (e.g., Duan et al., 2010).

Isotope ratio measurements were performed on a Thermo Neptune multi-collector ICPMS (MC-ICPMS) in low-resolution mode with an Elemental Scientific Inc. Apex inlet system and using sample-standard bracketing. All measurements were made using the Johnson Matthey Specpure Mo plasma standard (Lot #802309E; RochMo2) as the bracketing standard and then re-calculated relative to the new international NIST SRM 3134 standard = +0.25‰ (Nägler et al., 2014). In brief, the measured value for NIST SRM 3134 was 0.33 ± 0.04‰; 2SD relative to RochMo2 during our analytical sessions (Table 1). Accordingly, 0.08‰ was subtracted from each sample Mo isotope composition measured relative to RochMo2. Samples and standards were analyzed at a concentration of 25 ng/g Mo, which yielded about three volts of signal on mass 98. Samples were analyzed in duplicate (at least), with the average 2SD sample reproducibility being 0.05‰ and the maximum being 0.22‰. Over the period of Mo isotope analysis for this study, USGS rock reference material SDO-1 (Devonian Ohio Shale) was simultaneously processed with each batch of samples to monitor accuracy and showed good reproducibility (δ^{98}Mo = 1.07 ± 0.05‰; 2SD; compared to 1.05 ± 0.14‰; 2SD; in previous work [Goldberg et al., 2013]) as did multiple secondary standard solutions (Table 1). Lastly, for each analytical run, a series of standards with varying spike-sample ratios was measured. All samples were within the validated spike-sample range for accurate and precise δ^{98}Mo values.

3. RESULTS

Molybdenum isotope compositions in shales of the Doushantuo Formation from all slope and basin sections across the purported OOEs (i.e., in Doushantuo Members II, III, and IV) are predominantly negative (as low as -2.24 ± 0.10‰; 2SD; in Member II of the Taoying section) (Figs. 3 and 4). The heaviest measured shale δ^{98}Mo during the OOEs is 1.32 ± 0.15‰ (2SD) and comes from Member IV of the Rongxi section. Maximum δ^{98}Mo in shales deposited during the older OOEs are isotopically lighter: 0.76 ± 0.10‰ during the OOE in lower Member II (again from the Rongxi section) and 0.78 ± 0.10‰ during the OOE in lower Member III (from the Taoying section).

Table 1
Mo isotope data from standard reference material solutions.

Standard	δ^{98}Mo (2SD)[a], *	N	Normalized to NIST + 0.25‰*	Goldberg et al. (2013)
ICL-Mo	0.18 (0.04)	21	0.10 (0.04)	0.09 (0.05)
Kyoto-Mo	−0.03 (0.06)	5	−0.11 (0.06)	−0.12 (0.06)
NIST SRM 3134	0.33 (0.04)	42	0.25	0.25
SDO-1	1.14 (0.05)	35	1.06 (0.05)	1.05 (0.14)

* all reported errors are 2SD of the standard reproducibility.
[a] Measured relative to Roch-Mo2.

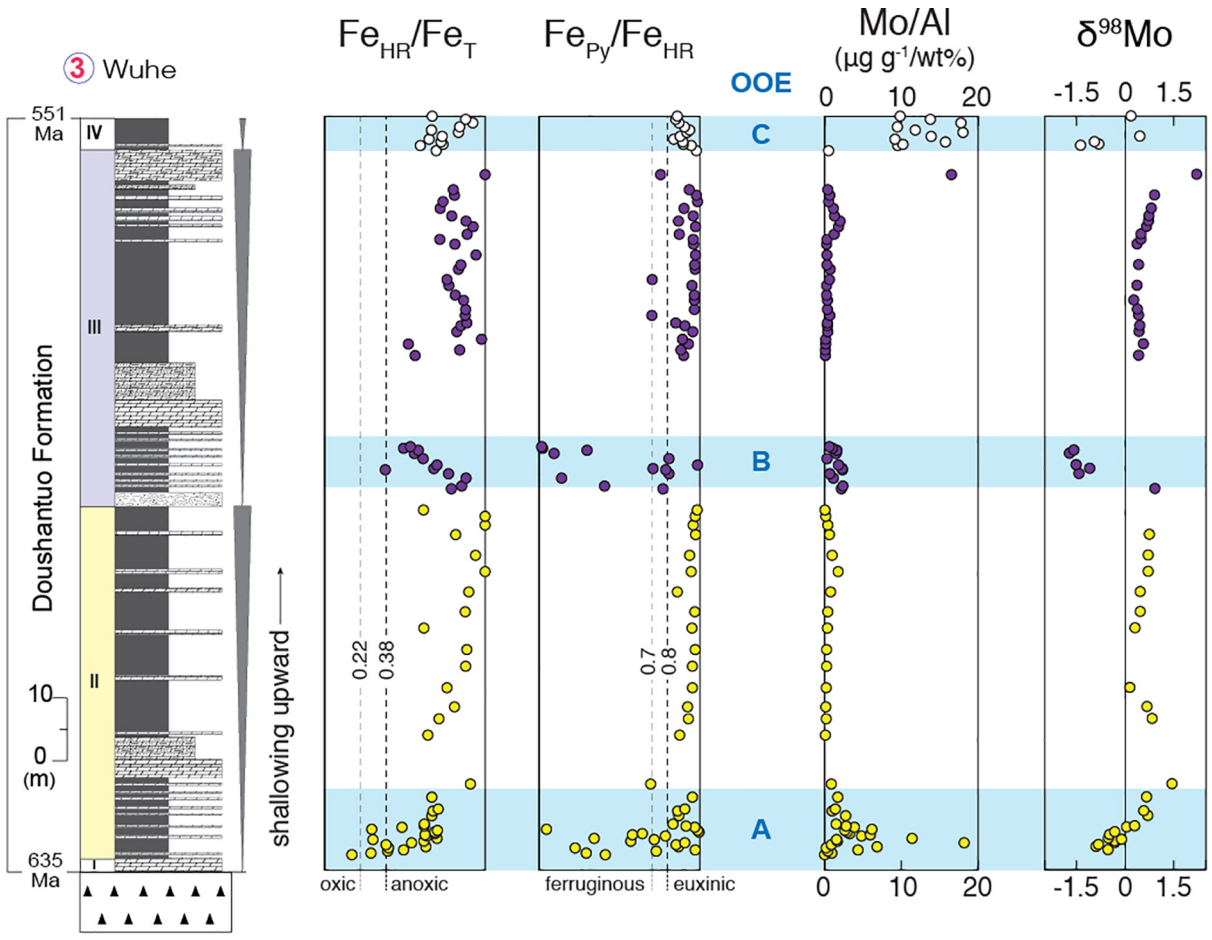

Fig. 3. Geochemistry of the Wuhe section. Iron speciation and trace metal data is from Sahoo et al. (2012, 2016). Thresholds for anoxic and euxinic deposition are adapted from Raiswell et al. (2018). Again, blue boxes signify purported OOEs. Data points are color-coded according to Doushantuo Member. See Fig. 1 for a lithology key. All error bars represent the 2SD reproducibility of that sample or the external long-term reproducibility of natural reference materials, whichever is greater. In most cases, error bars are smaller than the data points. Figure modified from Sahoo et al. (2016). (For interpretation of the references to color in this figure legend, the reader is referred to the web version of this article.)

In contrast, δ^{98}Mo in shales from the Wuhe section between the OOEs are always positive (Fig. 3). One sample from uppermost Member III from this section (110.7 m) is especially heavy (2.24 ± 0.10‰; 2SD). Other than this one sample, δ^{98}Mo values are much lighter, exceeding 1.0‰ only one other time (1.47 ± 0.10‰; 2SD; in lowermost Member II immediately above the oldest OOE) and remain fairly invariant otherwise (δ^{98}Mo = 0.57 ± 0.21‰; 2SD).

4. DISCUSSION

In the following section, we begin by first discussing local processes in the Ediacaran Nanhua Basin that most likely played a role in driving the observed negative Mo isotope compositions in the Doushantuo Formation (Section 4.1). We then discuss how these local processes likely also played some role in governing the RSE patterns

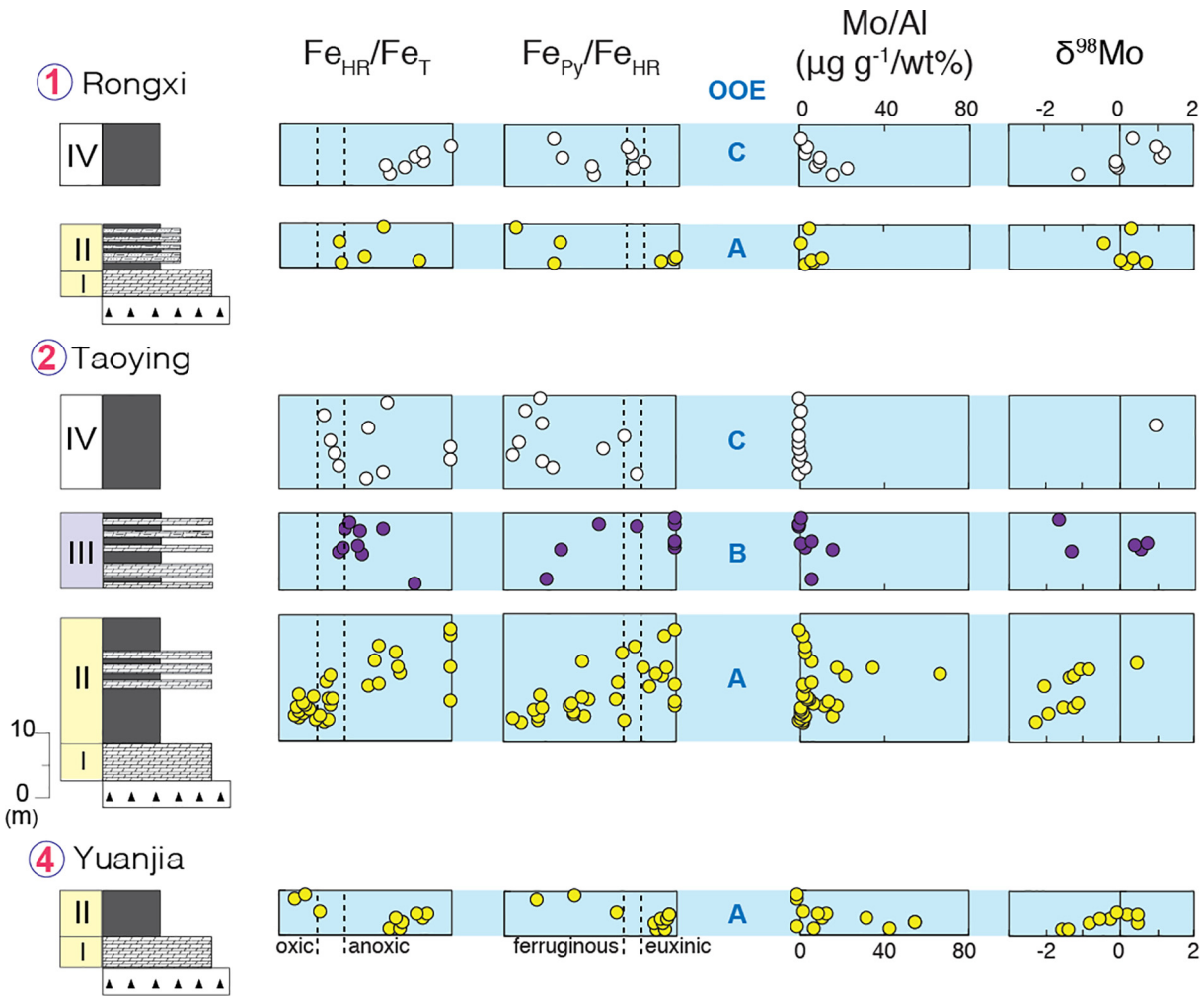

Fig. 4. Geochemistry of the Rongxi, Taoying, and Yuanjia sections. Iron speciation and trace metal data is from Sahoo et al. (2012, 2016) and Sahoo (2015). Thresholds for anoxic and euxinic deposition are adapted from Raiswell et al. (2018). Again, blue boxes signify purported OOEs and data points are color-coded according to Doushantuo Member. See Fig. 1 for a lithology key. All error bars represent the 2SD reproducibility of that sample or the external long-term reproducibility of natural reference materials, whichever is greater. In most cases, error bars are smaller than the data points. Figure modified from Sahoo et al. (2012). (For interpretation of the references to color in this figure legend, the reader is referred to the web version of this article.)

found in shales of the Doushantuo Formation (Section 4.2). Lastly, we finish this section by discussing a combination of plausible scenarios that may account for the transient nature of the geochemical excursions found in the Doushantuo Formation (Sections 4.3 and 4.4).

4.1. Negative δ^{98}Mo in Doushantuo shales

Negative δ^{98}Mo that are well below crustal estimates cannot represent Ediacaran global open-ocean seawater. The estimated average δ^{98}Mo of upper crustal rocks covers a restricted range between about 0.35‰ and 0.60‰ (Willbold and Elliot, 2017). Because the vast majority of Mo delivered to the ocean is sourced from crustal rocks (Miller et al., 2011; Greaney et al., 2018) and because all processes that operate during Mo delivery to and removal from the ocean preferentially retain lighter-mass Mo isotopes, the seawater δ^{98}Mo at any time in Earth's history was probably never lighter than this crustal composition (reviewed in Kendall et al., 2017).

Only two processes in modern marine settings are capable of driving the large negative Mo isotope fractionation effects observed in the Doushantuo Formation: delivery of lighter-mass Mo isotopes to sediments by (1) Mn oxide minerals (i.e., a Mo shuttle [Scholz et al., 2013, 2018]) and (2) thiomolybdates (Tossell, 2005; Neubert et al., 2008). The operation of one or both of these processes in the Ediacaran Nanhua Basin must have led to the preservation of a sedimentary δ^{98}Mo much lighter than the ancient seawater composition.

4.1.1. "Shuttling" by Mn oxide minerals

The transient development of a Mn oxide "shuttle" in the Ediacaran Nanhua Basin could help explain the negative δ^{98}Mo excursions in shales from the Doushantuo Formation. Today, the most well-studied marine basin hosting

a Mn oxide shuttle is the Baltic Sea (e.g., Scholz et al., 2013, 2018; Hardisty et al., 2016). In the Baltic Sea, during transient introduction of well-oxygenated waters into the semi-restricted basin, insoluble Mn oxides form high in the water column and sink to the seafloor (Huckriede and Meischner, 1996). Upon being introduced to the anoxic and euxinic conditions deeper in the water column or underlying sulfidic sediments, these same Mn oxides are solubilized during reductive dissolution, typically evading burial in marine sediments if O_2 is not present in bottom waters (Calvert and Pedersen, 1996; Häusler et al., 2018). Some RSEs bound to Mn oxides are retained in sediments after reductive dissolution, however, because they are less soluble under the reducing conditions present in bottom waters and sediments (e.g., Mo and V [Morford et al., 2005; Scholz et al., 2011, 2013]). In the case of Mo, the presence of appreciable hydrogen sulfide is required to promote sedimentary retention (Crusius et al., 1996; Morford et al., 2005). When Mo is shuttled by Mn oxides from oxic surface waters of the Baltic Sea to underlying sulfidic sediments, these sediments have δ^{98}Mo nearly 3.0‰ lighter than the overlying seawater value (Scholz et al., 2013, 2018), similar to the equilibrium isotope effect imparted during Mo sorption to Mn oxides ($\Delta^{98}Mo = 2.7 \pm 0.1$‰ [Wasylenki et al., 2008]).

In comparison, sediments that receive lighter-mass Mo isotopes via an Fe oxide shuttle have an authigenic δ^{98}Mo only ~1.0‰ lighter than the overlying seawater value (e.g., those from the geologically recent Peruvian continental margin [Scholz et al., 2017]). This smaller isotopic offset is similar to that imparted during Mo sorption to ferrihydrite and goethite ($\Delta^{98}Mo = 1.11 \pm 0.15$‰ and $\Delta^{98}Mo = 1.40 \pm 0.48$‰, respectively [Goldberg et al., 2009]), Fe oxide minerals shown to be abundant in particulate matter of the modern Peruvian margin oxygen minimum zone (Scholz et al., 2017). Given the magnitude of the δ^{98}Mo excursions found here in shales of the Doushantuo Formation (to as low as $\delta^{98}Mo_{NIST+0.25} = -2.24 \pm 0.10$‰; 2SD), it is unlikely that the sediments were strongly affected by an Fe oxide shuttle. More likely, the extremely light δ^{98}Mo require the larger Mo isotope fractionation effects associated with adsorption to Mn oxides ($\Delta^{98}Mo = 2.7 \pm 0.1$‰ [Wasylenki et al., 2008]).

Large V enrichments in shales from the Doushantuo Formation support the operation of an oxide shuttle in the Nanhua Basin. These shales are dramatically enriched in V (up to ~3 wt% [Sahoo et al., 2016]), more so than any modern marine sediments (all <0.05 wt% [Nameroff et al., 2002; Scholz et al., 2011]). In fact, the exceptional enrichments have been cited as challenging the original interpretation linking RSE enrichments to OOEs (Miller et al., 2017) and attributed instead to poorly understood secondary enrichment processes. Notably, V possesses a particularly strong affinity for oxide minerals and is consequently highly enriched in ferromanganese crusts (up to 0.08 wt% [Hein and Koschinsky, 2014]) relative to its abundance in seawater (35 nmol/L [Collier, 1984]), much more so than most other RSEs (Fig. 5). Modern anoxic marine sediments that receive RSE-laden oxides from overlying oxic waters, or those that form oxides in-situ during seasonal inflow of oxygenated waters, also become enriched in V (up to 0.04 wt% [e.g., Morford et al., 2005; Scholz et al., 2011]). A general negative correlation between V_{EF} and δ^{98}Mo ($R^2 = 0.59$; Fig. 6) is consistent with co-delivery of V and lighter-mass Mo isotopes via a Mn-oxide shuttle. This relationship is not as apparent between δ^{98}Mo and EFs for RSEs with a relatively lower affinity for oxide minerals (Mo_{EF} [$R^2 = 0.12$] and U_{EF} [$R^2 = 0.19$]; Fig. 6).

An alternate means of promoting V hyper-enrichment, recently proposed by Scott et al. (2017), is unlikely to have driven the strong V enrichments in the Doushantuo Formation. Scott et al. (2017) attribute strong V enrichments (up to 0.25 wt%) in organic-rich shales from the Late Devonian-Early Mississippian Bakken Formation to extremely high levels of H_2S (to >10 mM) in the original bottom waters or sediments. This hypothesis is supported by strong enrichment of Mo in the same shale samples (up to 0.18 wt%) because sedimentary Mo accumulation today is enhanced in H_2S-rich settings (Crusius et al., 1996; Morford et al., 2005). In the Doushantuo Formation, however, the most V-enriched shales (up to single wt% during OOE "B" in the Wuhe section; see Fig. 3) have very low Mo abundances (reaching only 15 ug/g). Furthermore, Fe speciation ratios in these shales, as well as those deposited during OOE "A" where V abundances are also very high (up to 0.4–0.6 wt% at the Taoying, Wuhe, and Yuanji sites), often dip below the thresholds for euxinic deposition (see Figs. 3 and 4). These geochemical fingerprints are inconsistent with the H_2S-replete conditions required by the Scott et al. (2017) hypothesis. Therefore, although this mechanism of V hyper-enrichments may explain the Bakken Formation data, it is not supported by the geochemical trends in the Doushantuo Formation.

Operation of an oxide shuttle during the OOEs is also suggested when viewed using a more classical method of identification – that is, preferential sedimentary accumulation of Mo over U under sulfidic conditions (Algeo and Tribovillard, 2009). During the operation of a local oxide shuttle, Mo can accumulate in sulfidic marine sediments much more efficiently than U because scavenging of Mo by oxide minerals is stronger than scavenging of U by oxide minerals (apparent in Fig. 5). Consistent with this model, Mo enrichments in Doushantuo shales during the OOEs are sometimes much greater than U when δ^{98}Mo are very negative (Fig. 7). Some shale samples with very negative δ^{98}Mo do not exhibit this Mo-U enrichment pattern, however, requiring an alternative explanation (see Section 4.1.2).

Importantly, muted Mn contents in bulk shale samples throughout the Doushantuo Formation from all sections studied here do not preclude the shuttle hypothesis (never above 0.24 wt% Mn relative to the average upper continental crust value of 0.08 wt% [Rudnick and Gao, 2003]; see Supplementary Data Table). Although sedimentary RSE enrichments are an expected consequence of an oxide shuttle, sedimentary Mn accumulation is not. Manganese is highly soluble after reductive dissolution under anoxic or euxinic conditions (as Mn^{2+}) and does not readily form sulfide minerals (Burdige, 1993). A persistent presence of free

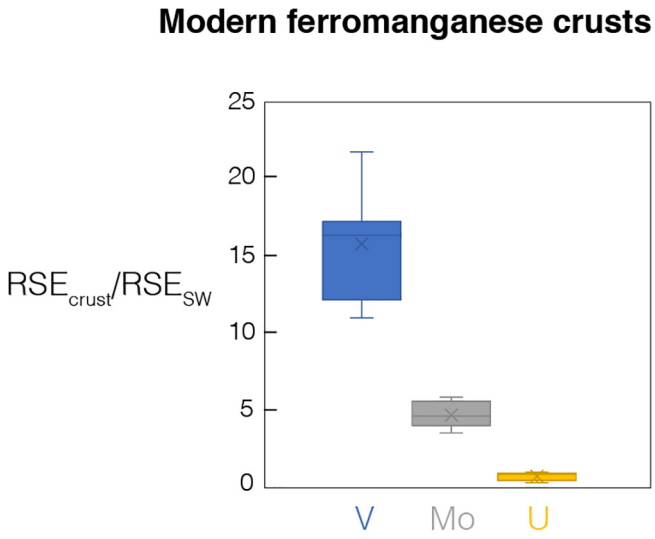

Fig. 5. Whisker plots showing relative abundance of redox-sensitive elements (RSEs) in modern seawater and ferromanganese crusts. Seawater RSE concentrations (in nmol/kg [Morris, 1975; Collier, 1984, and Chen et al., 1986]) and ferromanganese crust RSE abundances (in μg/g [Hein and Koschinsky, 2014]) come from previous work. Whisker plots represent the range of values when dividing the average RSE abundances from ferromanganese crusts from different sites (Table 1, Hein and Koschinsky [2014]) by the average seawater concentration of that RSE.

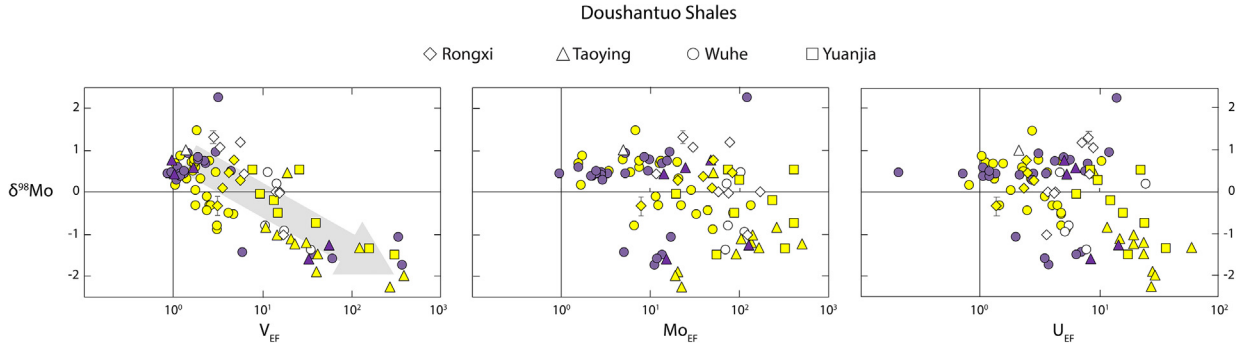

Fig. 6. Cross-plots of Mo isotope compositions and RSE enrichment factors (EF) in Doushantuo Shales. Mo isotope data is from this study and elemental abundances come from previous work (Sahoo et al., 2012, 2016). Enrichment Factors were calculated relative to upper continental crust as follows: $RSE_{EF} = (RSE/Al)_{shale} \div (RSE/Al)_{upper\ crust}$ (RSE abundances in μg/g and Al in wt%). Upper continental crust elemental abundances used in our calculations come from Rudnick and Gao (2003). Data point shapes coincide with the different sites from South China, and colors signify the different Doushantuo Members (II = yellow, III = purple, and IV = white). (For interpretation of the references to color in this figure legend, the reader is referred to the web version of this article.)

O_2 in marine bottom waters is required to promote appreciable Mn accumulation in marine sediments (Calvert and Pedersen, 1996; Häusler et al., 2018). Previous attempts to constrain local marine redox conditions on the slope of and within the deeper portions of the Nanhua Basin found evidence for either euxinic, anoxic, or suboxic conditions (e.g., Wang et al., 2012; Sahoo et al., 2012, 2016; Jin et al., 2018), all of which do not favor Mn accumulation. Even under the most oxidizing of these conditions (i.e., suboxic), O_2 may not sufficiently penetrate marine sediments to support Mn retention (Morford et al., 2005). Thus, there is no reason to expect Mn enrichments in shales of the Doushantuo Formation despite the likely delivery of Mo via Mn oxides. Notably, individual pyrite grains from shales of the Doushantuo Formation deposited during OOEs are slightly enriched in Mn (but <1.0 wt% [Gregory et al., 2017]). These slightly elevated abundances might fingerprint the intense (re)cycling of Mn that took place in the original bottom waters or sediments, especially given the low affinity of Mn for sulfide (Burdige, 1993).

4.1.2. Incomplete tetrathiomolybdate formation

When transfer of Mo from seawater into sediments is non-quantitative, a large isotopic offset can result from the formation of thiomolybdate ions (i.e., $MoO_xS_{4-x}^{2-}$), an offset that can leave sediments dramatically enriched in lighter-mass Mo isotopes (Tossell, 2005; Neubert et al., 2008; Nägler et al., 2011). Thiomolybdate ions form in the presence of hydrogen sulfide. In marine settings where hydrogen sulfide is abundant in marine bottom waters

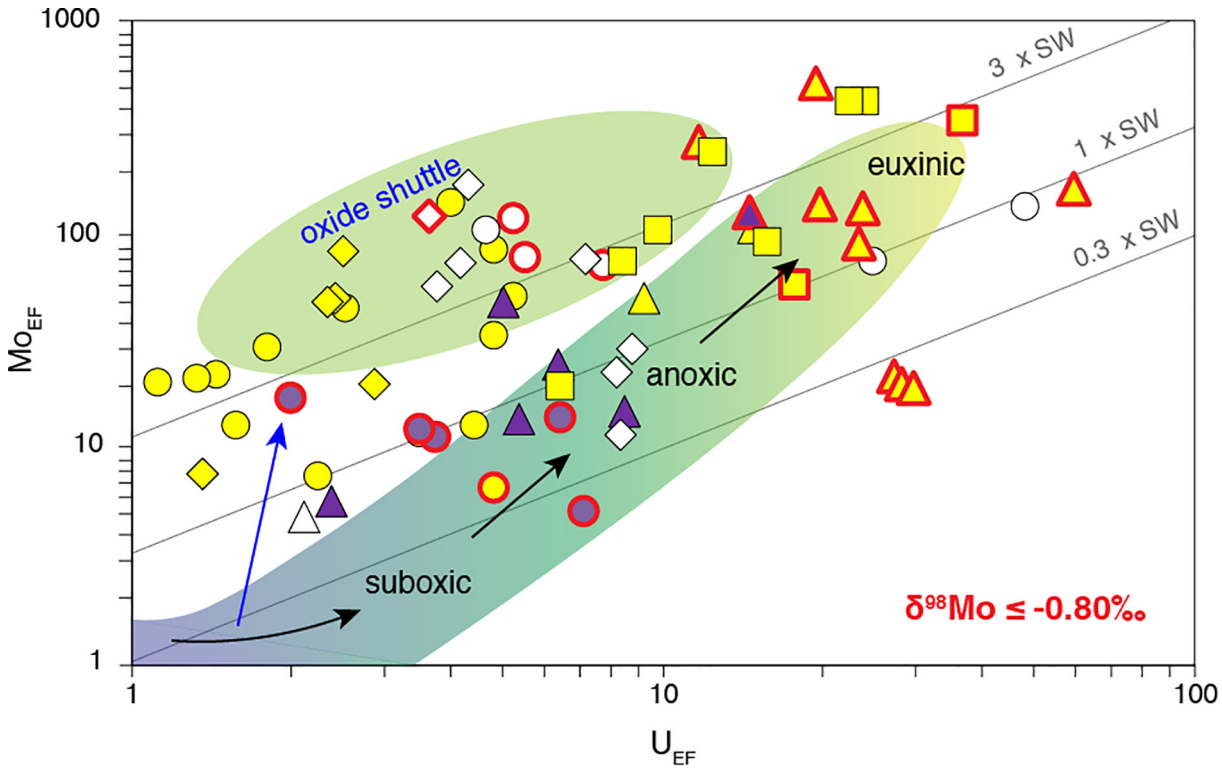

Fig. 7. Cross-plot of Mo and U enrichment Factors (EF) in Doushantuo Shales during OOEs. Trace metal data in this plot comes from Sahoo et al. (2012, 2016) and Sahoo (2015). Enrichment Factors were calculated relative to upper continental crust as follows: $RSE_{EF} = (RSE/Al)_{shale} \div (RSE/Al)_{upper\ crust}$ (RSE abundances in μg/g and Al in wt%). Upper continental crust elemental abundances used in our calculations come from Rudnick and Gao (2003). Data point shapes coincide with the different sites from South China (diamonds = Rongxi, triangles = Taoying, circles = Wuhe, and squares = Yuanjia) and colors signify the different Doushantuo Members (II = yellow, III = purple, and IV = white). Shale samples with $\delta^{98}Mo \leq -0.80‰$ are outlined in red. Figure and fields are modified from Algeo and Tribovillard (2009) and Jin et al. (2018). (For interpretation of the references to color in this figure legend, the reader is referred to the web version of this article.)

and sediments (>11 uM $H_2S_{(aq)}$), the predominant thiomolybdate formed is tetrathiomolybdate (MoS_4^{2-} [Erickson and Helz, 2000]). In marine settings where sulfide availability is low and/or unstable (i.e., where local marine bottom waters are only weakly or transiently euxinic, anoxic and non-sulfidic, or weakly oxygenated), however, conversion of molybdate to tetrathiomolybdate is incomplete and leads to the formation of thiomolybdate intermediates with very different Mo isotope compositions (mono- ($MoO_3S_1^{2-}$), di- ($MoO_2S_2^{2-}$), and tri- ($MoO_1S_3^{2-}$) thiomolybdates [Tossell, 2005]). In the most extreme case found to date, sedimentary $\delta^{98}Mo$ thought to be a product of incomplete tetrathiomolybdate formation are up to ~3‰ lighter than the seawater composition (immediately below the chemocline of the Black Sea [Neubert et al., 2008; Nägler et al., 2011]).

Similar to the identification of an oxide shuttle, variations in sedimentary Mo-U patterns may also be used to identify conditions unfavorable for quantitative tetrathiomolybdate transformation (e.g., Azrieli-Tal et al., 2014). Fluctuations in ancient localized hydrogen sulfide contents are thought to be fingerprinted in shales by progressive increases (more sulfidic) and decreases (less sulfidic) in the enrichments of both Mo and U (Algeo and Tribovillard, 2009). This pattern results from the shared affinity of both RSEs for reducing conditions, affinities that strengthen steadily as conditions become more reducing in marine bottom waters and sediments. Indeed, many of the Doushantuo shales with very negative $\delta^{98}Mo$ plot along a line of increasing Mo and U (Fig. 7). This relationship is an expected consequence of an ancient, relatively open-marine environment where redox conditions fluctuated between suboxic, anoxic, and euxinic deposition. Iron speciation ratios reported in previous work corroborate this suggestion (Sahoo et al., 2012, 2016). At times during the purported OOEs, Fe_{HR}/Fe_T and Fe_{Py}/Fe_{HR} ratios in all sections show variations consistent with deposition from oxic, anoxic, and euxinic bottom waters (Figs. 3 and 4). These variations in local redox conditions, particularly away from euxinia, would have promoted incomplete tetrathiomolybdate formation in the original sediments, resulting in the preferential retention of lighter-mass Mo isotopes.

Notably, some Doushantuo shale samples still plot outside of the suboxic-anoxic-euxinic and oxide shuttle fields in Fig. 7. Shales that plot between these two fields may be explained by some combination of fluctuations in local redox conditions (i.e., between suboxic, anoxic, and euxinic) and the operation of an oxide shuttle. The four shale samples from the Taoying site that plot to the right of the

suboxic-anoxic-euxinic field (i.e., those with much higher U_{EF} relative to Mo_{EF}; Fig. 7), however, may still require an alternative explanation. Nonetheless, with the exception of these four samples, all other Doushantuo shales plot within or between the suboxic-anoxic-euxinic and oxide shuttle fields. Therefore, the local processes these Mo_{EF}-U_{EF} patterns signify likely played the most significant role in driving the geochemical trends found in Doushantuo shales deposited during the purported OOEs.

4.2. A reappraisal of RSE trends in the Doushantuo Formation during OOEs

The processes outlined in the preceding section, in addition to driving light sedimentary $\delta^{98}Mo$, are known to have a profound effect on sedimentary RSE abundances. In this light, the RSE patterns in the Doushantuo Formation during the purported OOEs need to be re-assessed.

4.2.1. Links to other local processes in the Nanhua Basin

Sedimentary RSE enrichments today, in addition to being affected by oxide shuttling, are heavily dependent on local redox conditions. This dependency must have also been present in ancient marine sedimentary environments (summarized in Tribovillard et al., 2006). Of the RSEs highlighted here, V, Re, and U are all preferentially retained in sediments under anoxic conditions. Molybdenum, however, is not retained in sediments unless dissolved sulfide contents in marine bottom waters or sediment pore waters are comparatively high (Crusius et al., 1996; Morford et al., 2005). This well-documented link between Mo and sulfide is supported by the RSE data from the Doushantuo Formation during the OOEs. Specifically, Doushantuo shale samples with Fe_{HR}/Fe_T and Fe_{Py}/Fe_{HR} ratios indicative of euxinic deposition (i.e., $Fe_{HR}/Fe_T > 0.22$ and $Fe_{Py}/Fe_{HR} > 0.80$ [Raiswell et al., 2018]) have more pronounced Mo enrichments (in particular, shales from OOEs A and C; Fig. 8). These differences in the abundance of Mo between shales deposited under euxinic versus non-euxinic conditions (p-value = 0.000004 for a two-tailed and unpaired t-test) are greater than those observed for the other RSEs (p-value = 0.04 for U, 0.08 for V, and 0.12 for Re using the same test). Furthermore, Mo abundances are elevated in spheroidal pyrite grains throughout the Wuhe section, particularly during OOEs (Gregory et al., 2017). Together, these relationships support the idea that sedimentary Mo retention in the Doushantuo Formation was coupled to sulfide in the water column and sediments.

While, in general, shale Mo abundances during OOEs are greater when Fe speciation indicates deposition occurred under at least locally euxinic conditions, there are still clear exceptions to this rule. For example, a few shale samples deposited under euxinic conditions according to the Fe data possess very low Mo abundances (e.g., as low as 2 μg/g in the Wuhe section during OOE "B"), while some deposited under predominantly non-euxinic conditions based on the Fe data possess much higher Mo abundances (e.g., as high as 81 μg/g in the Rongxi section during OOE "C"). There are multiple possible explanations for these outliers. For example, local depositional controls in the paleo-basin, such as the availability and type of organic matter (Algeo and Lyons, 2006), sedimentary carbonate content, and sedimentation rates (Hardisty et al., 2018), would have influenced the sedimentary Mo abundances (as well as the other RSE abundances). Furthermore, each OOE represents roughly a duration of 5–10 million years (Sahoo et al., 2016). As such, fluctuations in global marine redox conditions within and especially between these events are possible, indeed likely, and could have played an important role in regulating sedimentary Mo abundances. Changes in the degree of connection between the Nanhua Basin and the open ocean, if this occurred over million-year timescales, would have also played a strong role in regulating the abundance of Mo in seawater and sediments of the basin (Algeo and Lyons, 2006).

4.2.2. Links to global ocean oxygenation

In modern marine sediments, Re and U, unlike Mo and V, are largely unaffected by oxide shuttling (Morford et al., 2005; Algeo and Tribovillard, 2009), and therefore their high abundances in black shales from the Doushantuo Formation are probably linked to extensive global ocean oxygenation. The only known way to enhance sedimentary Re and U abundances to Phanerozoic levels, such as is found during Ediacaran OOEs in the Doushantuo Formation, is by increasing ocean oxygenation and in turn expanding the size of their global seawater reservoirs (Partin et al., 2013; Sheen et al., 2018). This general relationship is evident in the ancient shale record, where both Re and U abundances are predominantly low in shales from the Precambrian but show a first-order increase across the Ediacaran-Cambrian boundary in response to an overall trend towards higher ocean O_2 levels in the Phanerozoic Eon (Partin et al., 2013; Sheen et al., 2018).

The combined effects of a local Mn oxide shuttle and global-scale OOEs may explain why sedimentary RSE enrichments in the Doushantuo Formation are so high, sometimes exceeding those found in modern marine sediments. Large-scale OOEs during the Ediacaran Period would have increased RSE reservoirs, while at the same time also stimulating RSE delivery to sedimentary environments hosting an oxide shuttle. These combined effects are apparent when shale V and Re abundances from the Doushantuo Formation during OOEs are plotted against one another and reveal a general correlation ($R^2 = 0.38$; Fig. 9). High sedimentary Re abundances in the Doushantuo Formation require global ocean oxygenation (Sheen et al., 2018), while high sedimentary V abundances may be best explained by supplementation via a local oxide shuttle (see Section 4.1.1). Therefore, the correlation between these two elements is an indication that both processes may have been operating in unison.

Molybdenum isotope compositions reported in this study for the Doushantuo Formation during the purported OOEs, despite the described complications and the exceptionally light values, could still be evidence for a better-oxygenated Neoproterozoic ocean. At multiple times during the Phanerozoic Eon, such as during some Mesozoic Oceanic Anoxic Events (OAEs), the seawater $\delta^{98}Mo$ is estimated to have been much lower than that of the modern

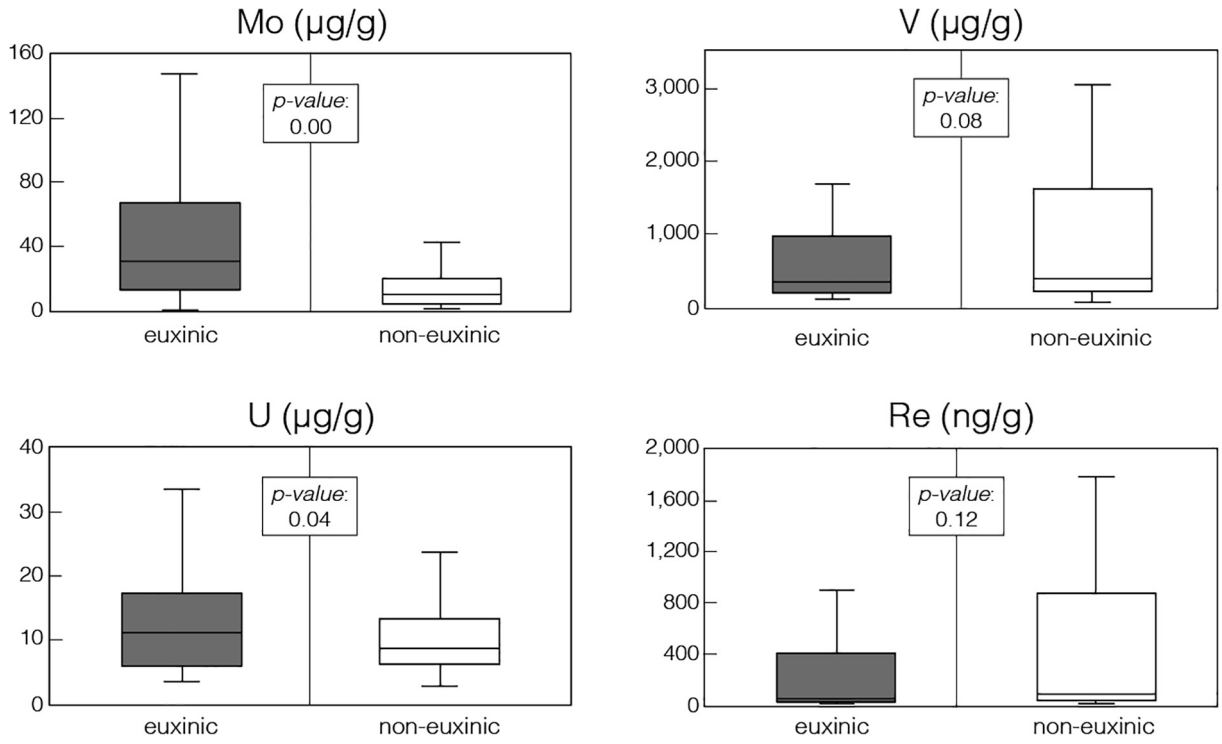

Fig. 8. Whisker plots showing RSE concentrations in Doushantuo shales during OOEs according to local redox conditions. Local redox conditions are determined by Fe speciation data (e.g., shale samples with $Fe_{HR}/Fe_T > 0.22$ and $Fe_{Py}/Fe_{HR} > 0.8$ are deemed euxinic in these plots). Data from all sections targeted in this study are included in the plots (i.e., Rongxi, Taoying, Wuhe, and Yuanjia). Iron speciation and RSE data is from Sahoo et al. (2012, 2016).

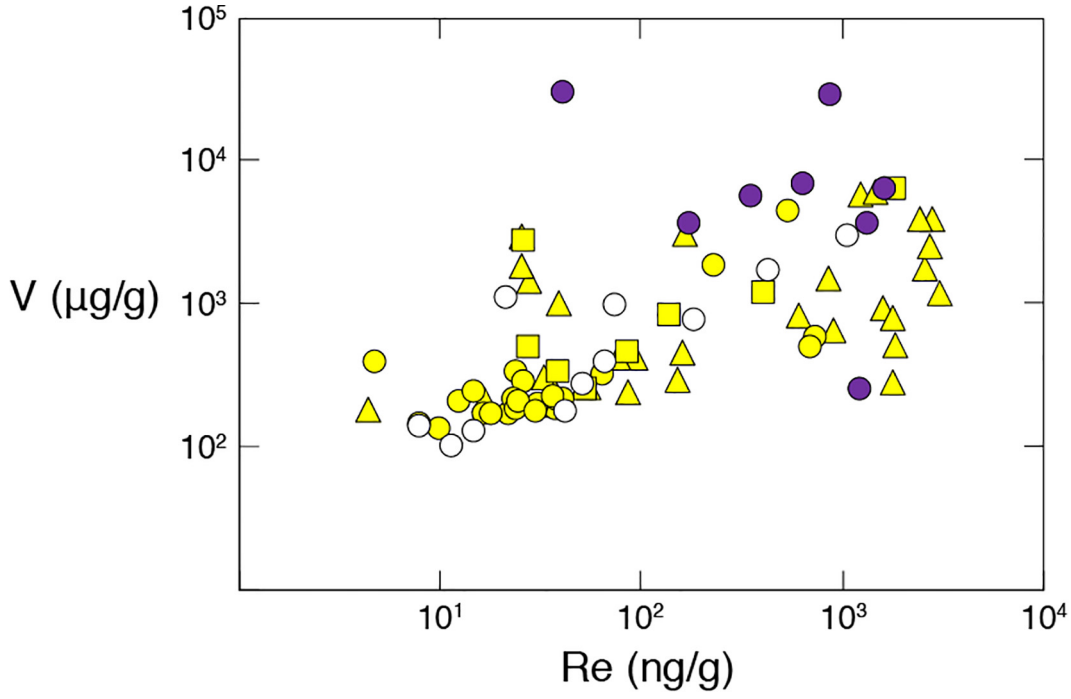

Fig. 9. Cross-plot of V and Re concentrations in Doushantuo Shales during OOEs. V and Re concentration data is from Sahoo et al. (2012, 2016). Data point shapes coincide with the different sites from South China (triangles = Taoying, circles = Wuhe, and squares = Yuanjia; similar to Fig. 6) and colors signify the different Doushantuo Members (II = yellow, III = purple, and IV = white). (For interpretation of the references to color in this figure legend, the reader is referred to the web version of this article.)

ocean ($\delta^{98}Mo_{SW} = \sim 1.45‰$ during both the Toarcian OAE and Cenomanian-Turonian OAE-2 [summarized in Dickson, 2017]). Paleoproxy evidence suggests that Earth's deep open ocean remained mostly oxygenated during these OAEs, with deoxygenation taking place primarily in shallow shelf and margin environments (<10% of the global seafloor [Owens et al., 2013; Dickson et al., 2016; Clarkson et al., 2018]). Large RSE enrichments are preserved in sedimentary rocks deposited during these events despite the large scale of marine deoxygenation and accompanying decline in seawater δ^{98}Mo (e.g., Mo concentrations in the hundreds of μg/g and V in the thousands [Hetzel et al., 2009; Owens et al., 2012; Owens et al., 2016]). In short, a seawater δ^{98}Mo during Ediacaran OOEs lower than that of the modern ocean is not inconsistent with the OOE hypothesis. Ocean oxygenation during the Ediacaran OOEs could have been greater than those present during most of the Proterozoic Eon – and perhaps comparable to ocean oxygenation levels during Mesozoic OAEs.

General agreement between the levels of predicted ocean oxygenation during Ediacaran OOEs and the Mesozoic OAEs could even be supported by the worldwide Neoproterozoic Fe speciation record (Sperling et al., 2015). When originally presented, these Fe data were interpreted in the opposite way – as being contradictory to the OOE hypothesis. Sperling et al. (2015) argued for predominantly anoxic global marine margins throughout the Neoproterozoic. These authors were limited to predictions for marine margin settings because Neoproterozoic shales on or near Earth's surface today were deposited predominantly in these proximal and relatively shallow settings (that is, a preservational bias leads to a sampling bias). During Mesozoic OAEs, pronounced ocean deoxygenation was most prevalent in marginal environments because of the higher biological production in these regions (Dickson et al., 2016; Owens et al., 2013; Owens et al., 2018). Therefore, in an ocean with redox conditions similar to those Mesozoic OAEs, margin settings may very well have been predominantly anoxic, despite increasing oxygenation away from those margins. If correct, this model would allow for the persistence of anoxia suggested in the Sperling et al. (2015) data along the margins, while still allowing for a well-oxygenated deep open ocean.

4.3. Transiency of negative δ^{98}Mo and strong RSE enrichments

Equally impressive as the magnitude of negative δ^{98}Mo and RSE enrichments in shales of the Doushantuo Formation is their transient and seemingly episodic appearance. The short-lived nature of these excursions (<5–10 million years [Sahoo et al., 2016]) may fingerprint major changes that occurred to the Nanhua Basin if not the global ocean during the Ediacaran.

We present two hypotheses: the transient nature of the geochemical trends found in the Doushantuo Formation may have been a result of some combination of (1) changes in the position of the local chemocline and/or (2) dramatic changes in global sea level. Critically, neither of these hypotheses can at present be ruled out as a contributing factor to the episodic geochemical trends. Furthermore, these hypotheses are not mutually exclusive; changes in the position of the local chemocline can be modulated by global sea level changes. For these reasons, we highlight here the evidence in support of each hypothesis and discuss some of the associated implications.

4.3.1. Links to chemocline fluctuations

A deepening of the chemocline in the Nanhua Basin during OOEs could help explain the geochemical trends found in the Doushantuo Formation. Deepening of the chemocline would have exposed more sediments on at least the slope of the Nanhua Basin, and potentially sediments deposited deeper within the basin (i.e., at the Yuanjia site), to oxic or suboxic bottom waters (e.g., Han and Fan, 2015). Manganese oxide minerals formed in these bottom waters, as well as higher in the water column, could then have shuttled RSEs to the marine sediments. Again, because Mn contents are muted in all shale samples analyzed here, O_2 in marine bottom waters at the studied localities probably did not penetrate deep enough into underlying sediments to promote Mn retention in these settings (i.e., conditions in sedimentary pore waters probably only reached suboxic; see Section 4.1.1). An additional consequence of more oxidizing marine bottom waters above the original Nanhua Basin sediments would be a decrease in the availability of labile organic matter, which would have suppressed accumulation of sulfide in pore waters. By association, incomplete sedimentary tetrathiomolybdate formation could also have been promoted by deepening of the chemocline. The coupled effects from a local Mn oxide shuttle and incomplete tetrathiomolybdate formation, as a result of a deepening chemocline in the Nanhua Basin, could have promoted retention of lighter-mass Mo isotopes in the original sediments.

Deepening of the chemocline during OOEs need not have been restricted to the Nanhua Basin, and instead this phenomenon may have occurred over large areas of Ediacaran global oceans. In fact, the original OOE hypothesis predicts this based on the requirement of enhanced global ocean oxygenation to drive the dramatic increase in each seawater RSE reservoir (Sahoo et al., 2012, 2016). Proterozoic oceans are thought to have been predominantly anoxic, with oxic conditions restricted primarily to shallow settings (e.g., Reinhard et al., 2013, 2016). In comparison, Ediacaran oceans during OOEs are thought to have been better oxygenated, with oxic conditions being commonly present also in much deeper settings.

If the local chemocline did deepen in the Ediacaran Nanhua Basin during the purported OOEs, then this phenomenon may have been linked to localized physical processes. For example, strengthened wind speeds can drive deeper local pycnoclines, and by extension also deeper chemoclines. Likewise, the formation of local bottom waters could have driven the same effect because, since these waters would have been very dense and O_2-rich, they would have introduced O_2 to greater depths in the water column (as has happened multiple times over the past few decades in areas of the Mediterranean Sea [Schneider et al., 2014]). The transient development of one or both

of these localized physical processes in the Ediacaran Nanhua Basin may therefore have been a major factor in driving the negative δ^{98}Mo excursions and coeval RSE patterns found in the Doushantuo Formation.

4.3.2. Links to changes in global sea level

The episodic geochemical trends found in the Doushantuo Formation could also have been stimulated by global sea level change during the Ediacaran. Marine regressions and transgressions show a strong link to the geochemical trends in the Doushantuo Formation (apparent in Fig. 3), and these dramatic changes in sea level have been invoked in previous work to explain other geochemical patterns in the Doushantuo Formation (Och et al., 2016).

Some of the geochemical trends found between the purported OOEs in Doushantuo shales from the Wuhe section, although not originally interpreted in this manner (Sahoo et al., 2016), could be linked to a loss in connection between the Nanhua Basin and the open ocean. A prevalence of the clay mineral saponite in sedimentary rocks from the Jiulongwan section from South China was interpreted as evidence for a shelf lagoon in the Nanhua Basin (see Fig. 1) that was strongly restricted during deposition of Members I and II of the Doushantuo Formation (Bristow et al., 2009; but also see Huang et al., 2013 for an alternative explanation of this data). Anomalously low RSE concentrations in sedimentary rocks of the Jiulongwan section (Mo and U abundances of ~2 μg/g) were interpreted as corroborative evidence for a restricted setting with limited RSE input from open ocean seawater (Bristow et al., 2009). Similar to the findings of Bristow et al. (2009), RSE abundances in the Wuhe section outside of the purported OOEs are also extremely low (Mo and U, for example, are often <2 μg/g [Sahoo et al., 2016]) and may thus be interpreted in the same way. Importantly, the degree of restriction on the slope and in the deeper basin need not have been as severe as that experienced by the shelf lagoon. Isolation of the shelf lagoon during deposition of Members I and II of the Doushantuo Formation is postulated to have been sufficiently strong to promote a lacustrine environment (Bristow et al., 2009; but also see Huang et al., 2013), but coeval sections at this time deposited in the basin probably maintained some connection to the open ocean (Bristow et al., 2009).

Evidence for a semi-restricted Nanhua Basin between the purported OOEs is not limited to low RSE abundances. For instance, local reservoir effects in highly restricted euxinic environments today with very low seawater sulfate concentrations prevent transfer of the large negative S isotope fractionation effects induced during microbial sulfate reduction to sediments of those basins (Gomez and Hurtgen, 2015). Positive pyrite S isotope compositions between OOEs in the Wuhe section (Sahoo et al., 2016) could therefore also be explained by the development of basinal restriction. Basinal restriction may also help explain why sediments from the Wuhe site were deposited under a persistently euxinic water column between the OOEs (according to Fe speciation data; Fig. 3). Modern restricted basins where inflow of nutrient- and O_2-rich marine bottom waters is limited are also often euxinic (Meyer and Kump, 2008). It is worth noting, however, that modern restricted basins are probably more susceptible to the development of euxinic conditions than were restricted basins during the Ediacaran because of the higher abundance of sulfate in modern seawater. Furthermore, a strong surface-to-deep carbon (C) isotope gradient in the Ediacaran Nanhua Basin between the OOEs has been inferred from systematic differences in the carbonate and organic C isotope profiles from various sections in South China (e.g., Jiang et al., 2007; Wang et al., 2016). Strong surface-to-deep C isotope gradients are found today in restricted redox-stratified basins (e.g., the Black Sea and Framvaren Fjord [Volkov, 2000]). Finally, independent evidence for regression and development of sea-level lowstands (e.g., the appearance of cross-laminations in carbonates from South China [McFadden et al., 2008]) coincides with the periods between OOEs (apparent in Fig. 3) and may have favored basin restriction. Many basins are likely to lose at least some connectivity with the open ocean during sea level lowstands.

Like the correlation between marine regressions and the intervals between the OOEs, the correlation between marine transgressions and the OOEs themselves may also not be coincidental. In fact, marine transgression, by improving connection between the Ediacaran Nanhua Basin and the open ocean, provides a means of catalyzing a vigorous Mn oxide shuttle and bringing metals into the basin. In the modern Baltic Sea, the operation of a Mn oxide shuttle is catalyzed in a similar manner – that is, by the transient introduction of well-oxygenated waters into the semi-restricted basin (Huckriede and Meischner, 1996). We propose that times of transient inflow of well-oxygenated Ediacaran ocean surface waters to a Nanhua Basin that was better connected to the open ocean stimulated a Mn oxide shuttle similar to that observed in the modern Baltic Sea. During these inflow events, rapid accumulation of isotopically light Mo, as well as many other RSEs, would have occurred in euxinic sediments of the basin.

Some key differences do exist between the geochemistry of sediments from the recent Baltic Sea and that preserved in the Doushantuo Formation. For example, Mn contents reach much higher values in geologically recent Baltic Sea sediments compared to those of the Doushantuo Formation (~15 wt% [Hardisty et al., 2016] versus <1.0 wt% [Sahoo et al., 2016], respectively). We could explain this disparity by inflow events into the Ediacaran Nanhua Basin that were sporadic or of weaker intensity relative to those occurring recently in the Baltic Sea. The presence of O_2 in marine bottom waters and its ability to catalyze Mn oxide formation in underlying sediments is likely a prerequisite for sedimentary Mn accumulation (Calvert and Pedersen, 1996). In support of this assumption, sedimentary Mn accumulation in the Baltic Sea is limited during inflow events that occur sporadically over extremely short timescales (e.g., a single year) because penetration of O_2 into marine bottom waters occurs over correspondingly short timescales and leads to only limited Mn oxide formation (Heiser et al., 2001; Lenz et al., 2015). By analogy, Ediacaran sediments are not expected to have accumulated Mn if O_2 penetration into deep marine waters of the local sedimentary basin was sporadic or if O_2 failed to penetrate into the deep waters of the basin.

4.4. Implications of basinal restriction between the OOEs

A weakened connection between the Nanhua Basin and the open ocean during the intervals between the purported OOEs would have had profound consequences on the geochemistry of the basin. Today, a poor connection between the Black Sea and the open ocean inhibits delivery of Mo to this basin (Eckert et al., 2013). Consequently, the availability of Mo in bottom waters and also its burial flux in organic-rich sediments of the modern Black Sea are not as pronounced as those observed in anoxic basins better connected to the open ocean (e.g., the Cariaco Basin [Algeo and Lyons, 2006]). Knowing this, it becomes apparent that shale Mo abundances between the purported OOEs may undersell the true size of the coeval global seawater Mo inventory if the basin was poorly connected to the open ocean at these times. Additionally, it has been shown that organic-rich marine sediments from modern restricted basins such as the Black Sea (Neubert et al., 2008) are ideal candidates for capturing the contemporaneous seawater δ^{98}Mo (as well as Kyllaren fjord [Noordmann et al., 2015] and Lake Rogoznica [Bura-Nakić et al., 2018]). This is so because minimized recharge of Mo from the open ocean into these settings strengthens the possibility of near-quantitative Mo transfer from marine bottom waters to sediments. Therefore, although these sedimentary enrichments may undersell the true size of the coeval global seawater Mo reservoir, shales deposited at these times may be ideal candidates for capturing the coeval global seawater δ^{98}Mo.

If shales deposited between the purported OOEs from the Wuhe site did faithfully capture the coeval seawater δ^{98}Mo, then that composition was generally very light ($\delta^{98}Mo_{SW} \leq 0.94 \pm 0.10‰$; 2SD). We indicate "generally" because our low-resolution study of shales at the Wuhe site (one sample about every two meters) is very likely to leave large expanses of Ediacaran time unaccounted for – millions of years in some cases, based on sample age estimates from Sahoo et al. (2016). Furthermore, two shale samples from the Wuhe site that may have been deposited outside of the OOEs have heavier δ^{98}Mo ($1.47 \pm 0.10‰$; 2SD at 13.7 m and $2.24 \pm 0.10‰$; 2SD at 110.7 m) and may signify short-lived increases to the coeval seawater δ^{98}Mo. Alternatively, these heavier δ^{98}Mo may actually be from shale samples deposited near the termination or shortly after the onset of the OOEs. This scenario is possible because the two shale samples from Wuhe with comparatively heavy δ^{98}Mo are located immediately before or after the purported OOEs (according the OOE locations proposed in Sahoo et al. [2016]; Fig. 3). Nevertheless, generally lighter seawater δ^{98}Mo estimates inferred from the vast majority of shales deposited outside of the OOEs may indicate generally lower global ocean O_2 contents at these times.

5. CONCLUSIONS

Our new Mo isotope data help us argue that local controls in the Ediacaran Nanhua Basin played important roles in driving some of the geochemical trends in black shales of the Doushantuo Formation from South China. In particular, the transient development of an Mn oxide shuttle and changes in the extent of tetrathiomolybdate formation linked to sulfide availability are both supported by the extremely negative shale δ^{98}Mo excursions reported here. Coeval RSE patterns and accompanying Fe speciation data from the same sedimentary rocks, although not originally interpreted in this manner (Sahoo et al., 2012, 2016), are also consistent with this hypothesis.

Importantly, enhanced oceanic oxygenation during the Ediacaran is still required to explain some of the geochemical patterns in the Doushantuo Formation (i.e., those found in Sahoo et al., 2012, 2016), despite the local redox-related complications identified here. Elevated Re and U abundances are particularly difficult to explain without invoking global-scale oceanic oxygenation because oxide shuttling and changes in local sulfide availability are not adequate to enrich these two metals to the levels found in the Doushantuo Formation.

In light of our new data, it is worth reconsidering whether the Nanhua Basin maintained an uninterrupted connection with the open ocean during the entirety of the Ediacaran Period. If the Nanhua Basin was well-connected to the open ocean throughout the Ediacaran (as is assumed in previous work [Sahoo et al., 2012, 2016]), then:

(1) Redox-sensitive element abundances in organic-rich shales from the Doushantuo Formation should scale with coeval levels of global ocean oxygenation. Elevated RSE abundances would signify a better oxygenated global ocean, while muted RSE abundances would be indicative of a relatively less oxygenated one (i.e., the original hypothesis of Sahoo et al. [2016]);
(2) Negative δ^{98}Mo excursions are likely a consequence of chemocline deepening in the basin (Section 4.3.1.; and also see the leftmost panels in Fig. 10). When the chemocline deepened, more sediments on the slope of the basin would have been exposed to oxic or suboxic conditions. Shuttling of Mo to sediments by Mn oxides would be more likely under these conditions. Sedimentary sulfide contents may also have diminished under these conditions, in turn promoting incomplete tetrathiomolybdate formation. Both of these processes are known to stimulate retention of lighter-mass Mo isotopes in marine sediments and may thus explain the negative δ^{98}Mo.
(3) Positive δ^{98}Mo found in organic-rich euxinic shales deposited between the OOEs are likely a consequence of chemocline shallowing. When the chemocline shallowed, more sediments on the slope of the basin would have been exposed to euxinic conditions. Shuttling of Mo to sediments by Mn oxides would have been less likely under these conditions. An associated increase in local sulfide availability would have also favored more complete tetrathiomolybdate formation. Neither of these processes would have favored the retention of lighter-mass Mo isotopes in marine sediments. The positive δ^{98}Mo in these shales are most likely closer to matching the coeval ancient sea-

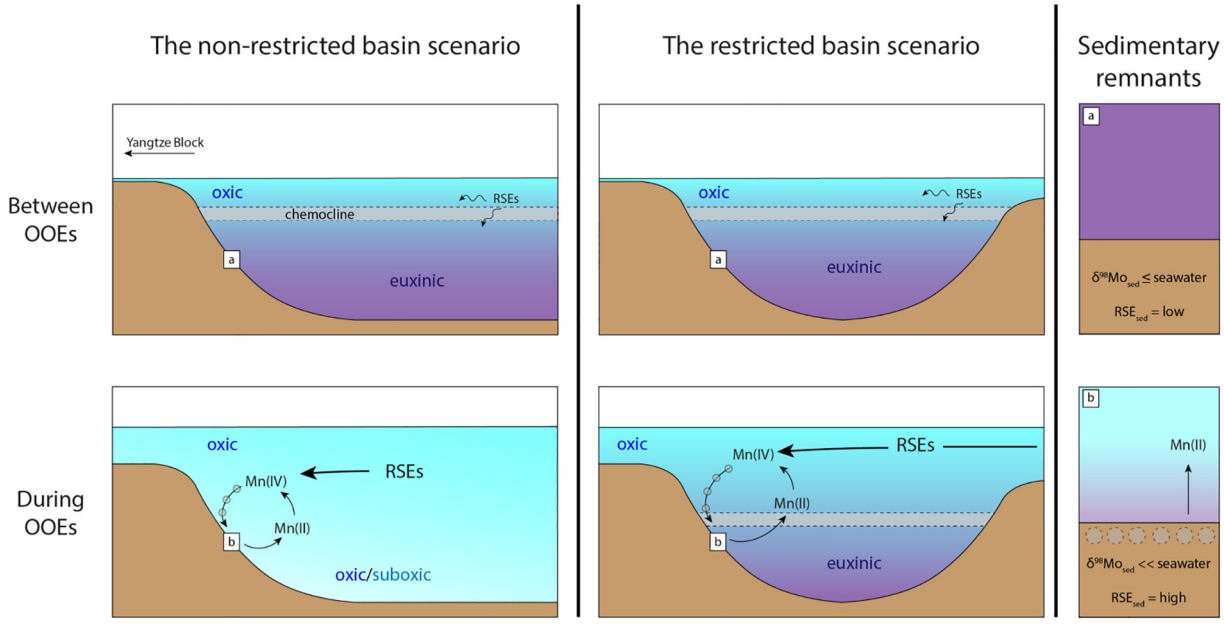

Fig. 10. Possible evolution of seawater in the Ediacaran Nanhua Basin depending on the degree of connection between this basin and the open ocean. The leftmost panels outline the possible evolution of seawater if the Nanhua Basin maintained an uninterrupted connection with the open ocean throughout the Ediacaran. The center panels outline this possible evolution if the Nanhua Basin was at times a restricted basin. Panels at the far right labeled "a" and "b" outline the associated sedimentary remnants on the slope of the paleo basin for each scenario (a = between OOEs and b = during OOEs). Grey circles represent insoluble Mn oxide minerals.

water composition. Unfortunately, it is difficult to tell if the true seawater δ^{98}Mo is recorded. Modern marine basins that maintain a strong connection with the open ocean never capture the coeval seawater δ^{98}Mo and instead capture a large range of isotopically lighter values (summarized by Kendall et al., 2017). By analogy, the organic-rich shales of the Doushantuo may also capture fractionated Mo isotope values.

Alternatively, if the connection between this basin and the open-ocean was not always strong during the Ediacaran (Section 4.3.2.; and also see the center panels in Fig. 10), then:

(1) Organic-rich shales of the Doushantuo Formation deposited during sea level highstands would be the best candidates to preserve the remnants of open-ocean chemistry, as viewed from the perspective of RSE enrichments. This likelihood is because the Nanhua Basin would have been most strongly connected to the open ocean at these times. By contrast, muted RSE enrichments in shales deposited during sea level lowstands would not be as likely to preserve information about the RSE reservoir of the open-ocean. This possibility is especially true if the Nanhua Basin was at times strongly restricted and exchanged little or no seawater with the open ocean.
(2) Negative δ^{98}Mo excursions are likely a consequence of open-ocean seawater inflow events into an otherwise restricted basin – similar to what happens today in the Baltic Sea (Scholz et al., 2018). During transgressions, inflow of oxic open-ocean surface waters to the basin could have stimulated the operation of a local Mn oxide shuttle, while also exposing more sediments on the slope to oxic or suboxic conditions. Again, lighter-mass Mo isotopes would be preferentially retained in sediments due to these processes.
(3) Positive δ^{98}Mo found in organic-rich shales during marine regressions are, again, primarily a result of the termination of the processes driving the extremely negative δ^{98}Mo excursions. However, if these shales were deposited in a strongly restricted basin, then they are strong candidates to preserve the coeval seawater δ^{98}Mo because restricted euxinic basins are shown to sometimes capture the coeval seawater δ^{98}Mo today (Neubert et al., 2008; Noordmann et al., 2015; Bura-Nakić et al., 2018). The majority of seawater δ^{98}Mo inferred from these shales ($\delta^{98}Mo_{SW} \leq 0.94 \pm 0.10‰$; 2SD) are much lighter than that of the modern ocean ($\delta^{98}Mo_{SW} = 2.34 \pm 0.10‰$ [Nägler et al., 2014]). Accordingly, these lighter δ^{98}Mo may fingerprint a comparatively less oxygenated global ocean at that time compared to the modern ocean.

Some combination of both scenarios could also explain the data.

Moving forward, it will be important to unmix or at least account for these local and global complications and their links to geochemical trends in Ediacaran-aged sedimentary rocks. Constraining the degree of restriction between the Ediacaran Nanhua Basin and the open ocean during the time intervals between the purported OOEs is of particular importance. To date, inferences about the

state of global marine redox conditions during the Ediacaran are based mostly on geochemical trends found in shales of the Doushantuo Formation and their relationship to coeval open-ocean chemistry. Well-documented contemporaneous shales from the multiple sections of Northwestern Canada (e.g., Johnston et al., 2013; Miller et al., 2017) are another potentially attractive target for future paleoredox studies. However, the Ediacaran-aged shales from Northwestern Canada offer their own challenges because they are thought to have been deposited under primarily ferruginous conditions (based on Fe speciation data [Johnston et al., 2013; Miller et al., 2017]), which limits the utility of paleoredox proxies such as Mo.

ACKNOWLEDGEMENTS

We would like to thank Wang Zheng for his help with instrumental analysis at Arizona State University. This research was supported financially by the NSF Frontiers in Earth System Dynamics program award NSF EAR-1338810 (C.M.O., T.W.L., and A.D.A.), the Natural Sciences and Engineering Research Council of Canada (NSERC) Discovery Grant RGPIN-435930 (B.K.), the Earth-Life Transitions Program of the U.S. National Science Foundation (T.W.L. and N.J.P.) and the NASA Astrobiology Institute under Cooperative Agreement No. NNA15BB03A issued through the Science Mission Directorate (T.W.L, N.J.P., and A.D.A.). This material is based upon work supported by the National Science Foundation Graduate Research Fellowship Program under Grant No. 026257-001 (C.M.O.). Any opinions, findings, and conclusions or recommendations expressed in this material are those of the authors and do not necessarily reflect the views of the National Science Foundation.

APPENDIX A. SUPPLEMENTARY MATERIAL

Supplementary data to this article can be found online at https://doi.org/10.1016/j.gca.2019.07.016.

REFERENCES

Algeo T. J. and Lyons T. W. (2006) Mo-total organic carbon covariation in modern anoxic marine environments: Implications for analysis of paleoredox and paleohydrographic conditions. *Paleoceanography* **21**, PA1016.

Algeo T. J. and Tribovillard N. (2009) Environmental analysis of paleoceanographic systems based on molybdenum-uranium covariation. *Chem. Geol.* **268**, 211–225.

An Z., Jiang G., Tong J., Tian L., Ye Q., Song H. and Song H. (2015) Stratigraphic position of the Ediacaran Miaohe biota and its constrains on the age of the upper Doushantuo $\delta^{13}C$ anomaly in the Yangtze Gorges area, South China. *Precambrian Res.* **271**, 243–253.

Arnold G. L., Anbar A. D., Barling J. and Lyons T. W. (2004) Molybdenum isotope evidence for widespread anoxia in Mid-Proterozoic oceans. *Science* **304**, 87–90.

Azrieli-Tal I., Matthews A., Bar-Matthews M., Almogi-Labin A., Vance D., Archer C. and Teutsch N. (2014) Evidence from molybdenum and iron isotopes and molybdenum-uranium covariation for sulphidic bottom waters during Eastern Mediterranean sapropel S1 formation. *Earth Planet. Sci. Lett.* **393**, 231–242.

Barling J., Arnold G. L. and Anbar A. D. (2001) Natural mass-dependent variations in the isotopic composition of molybdenum. *Earth Planet. Sci. Lett.* **193**, 447–457.

Bristow T. F., Kennedy M. J., Derkowski A., Droser M. L., Jiang G. and Creaser R. A. (2009) Mineralogical constraints on the paleoenvironments of the Ediacaran Doushantuo Formation. *Proc. Natl. Acad. Sci.* **106**, 13190–13195.

Bura-Nakić E., Andersen M. B., Archer C., de Souza G. F., Marguš M. and Vance D. (2018) Coupled Mo-U abundances and isotopes in a small marine euxinic basin: constraints on processes in euxinic basins. *Geochim. Cosmochim. Acta* **222**, 212–229.

Burdige D. J. (1993) The biogeochemistry of manganese and iron reduction in marine sediments. *Earth Sci. Rev.* **35**, 249–284.

Calvert S. E. and Pedersen T. F. (1996) Sedimentary geochemistry of manganese: Implications for the environment of formation of manganiferous black shales. *Econ. Geol.* **91**, 36–47.

Chen J. H., Edwards R. L. and Wasserburg G. J. (1986) 238-U, 234-U and 232-Th in seawater. *Earth Planet. Sci. Lett.* **80**, 241–251.

Clarkson M. O., Stirling C. H., Jenkyns H. C., Dickson A. J., Porcelli D., Moy C. M., Pogge von Strandmann P. A. E., Cooke I. R. and Lenton T. M. (2018) Uranium isotope evidence for two episodes of deoxygenation during Oceanic Anoxic Event 2. *Proc. Natl. Acad. Sci.*, 2918–2923.

Collier R. W. (1984) Particulate and dissolved vanadium in the North Pacific Ocean. *Nature* **309**, 441–444.

Condon D., Zhu M., Bowring S., Wang W., Yang A. and Jin Y. (2005) U-Pb ages from the Neoproterozoic Doushantuo Formation, China. *Science* **308**, 95–98.

Crusius J., Calvert S., Pedersen T. and Sage D. (1996) Rhenium and molybdenum enrichments in sediments as indicators of oxic, suboxic and sulfidic conditions of deposition. *Earth Planet. Sci. Lett.* **145**, 65–78.

Dickson A. J., Jenkyns H. C., Porcelli D., van den Boorn S. and Idiz E. (2016) Basin-scale controls on the molybdenum-isotope composition of seawater during Oceanic Anoxic Event 2 (Late Cretaceous). *Geochim. Cosmochim. Acta* **178**, 291–306.

Dickson A. J. (2017) A molybdenum-isotope perspective on Phanerozoic deoxygenation events. *Nat. Geosci.* **10**, 721–726.

Duan Y., Anbar A. D., Arnold G. L., Lyons T. W., Gordon G. W. and Kendall B. (2010) Molybdenum isotope evidence for mild environmental oxygenation before the Great Oxidation Event. *Geochim. Cosmochim. Acta* **74**, 6655–6668.

Eckert S., Brumsack H. J., Severmann S., Schnetger B., März C. and Fröllje H. (2013) Establishment of euxinic conditions in the Holocene Black Sea. *Geology* **41**, 431–434.

Erickson B. E. and Helz G. R. (2000) Molybdenum(VI) speciation in sulfidic waters: stability and lability of thiomolybdates. *Geochim. Cosmochim. Acta* **64**, 1149–1158.

Fike D. A., Grotzinger J. P., Pratt L. M. and Summons R. E. (2006) Oxidation of the Ediacaran ocean. *Nature* **444**, 744–747.

Gill B. C., Lyons T. W., Young S. A., Kump L. R., Knoll A. H. and Saltzman M. R. (2011) Geochemical evidence for widespread euxinic in the Later Cambrian ocean. *Nature* **469**, 80–83.

Goldberg T., Archer C., Vance D. and Poulton S. W. (2009) Mo isotope fractionation during adsorption to Fe (oxyhydr) oxides. *Geochim. Cosmochim. Acta* **73**, 6502–6516.

Goldberg T., Archer C., Vance D., Thamdrup B., McAnena A. and Poulton S. W. (2012) Controls on Mo isotope fractionations in a Mn-rich anoxic marine sediment, Gullmar Fjord, Sweden. *Chem. Geol.* **296–297**, 73–82.

Goldberg T., Gordon G., Izon G., Archer C., Pearce C. R., McManus J., Anbar A. D. and Rehkämper M. (2013) Reso-

lution of inter-laboratory discrepancies in Mo isotope data: an intercalibration. *J. Anal. Atomic Spectrom.* **28**, 724–735.

Gomez M. L. and Hurtgen M. T. (2015) Sulfur isotope fractionation in modern euxinic systems: implications for paleoenvironmental reconstructions of paired sulfate-sulfide isotope records. *Geochim. Cosmochim. Acta* **157**, 39–55.

Greaney A. T., Rudnick R. L., Gaschnig R. M., Whalen J. B., Luais B. and Clemens J. D. (2018) Geochemistry of Molybdenum in the continental crust. *Geochim. Cosmochim. Acta* **238**, 36–54.

Gregory D. D., Lyons T. W., Large R. R., Jiang G., Stepanov A. S., Diamond C. W., Figueroa M. C. and Olin P. (2017) Whole rock and discrete pyrite geochemistry as complementary tracers of ancient ocean chemistry: an example from the Neoproterozoic Doushantuo Formation, China. *Geochim. Cosmochim. Acta* **216**, 201–220.

Han T. and Fan H. (2015) Dynamic evolution of the Ediacaran ocean across the Doushantuo Formation, South China. *Chem. Geol.* **417**, 261–272.

Hardisty D. S., Riedinger N., Planavsky N. J., Asael D., Andren T., Jorgensen B. B. and Lyons T. W. (2016) A Holocene history of dynamic water column redox conditions in the Landsort Deep, Baltic Sea. *Am. J. Sci.* **316**, 713–745.

Hardisty D. S., Lyons T. W., Riedinger N., Isson T. T., Owens J. D., Aller R. C., Rye D. M., Planavsky N. J., Reinhard C. T., Gill B. C., Masterson A. L., Asael D. and Johnston D. T. (2018) An evaluation of sedimentary molybdenum and iron as proxies for pore fluid paleoredox conditions. *Am. J. Sci.* **318**, 527–556.

Häusler K., Dellwig O., Schnetger B., Feldens P., Leipe T., Moros M., Pollehne F., Schönke M., Wegwerth A. and Arz H. W. (2018) Massive Mn carbonate formation in the Landsort Deep (Baltic Sea): hydrographic conditions, temporal succession, and Mn budget calculations. *Mar. Geol.* **395**, 260–270.

Hein J. and Koschinsky A. (2014) Deep-ocean ferromanganese nodules and crusts. In *Treatise on Geochemistry 2nd Edition (TGC2), New Volume on Geochemistry of Mineral Deposits*, 2nd ed. (ed. S. Scott), pp. 273–291.

Heiser U., Neumann T., Scholten J. and Stüben D. (2001) Recycling of manganese from anoxic sediments in stagnant basins by seawater inflow: a study of surface sediments from the Gotland Basin, Baltic Sea. *Mar. Geol.* **177**, 151–166.

Hetzel A., Böttcher M. E., Wortmann U. G. and Brumsack H. (2009) Paleo-redox conditions during OAE 2 reflected in Demerara Rise sediment geochemistry (ODP Leg 207). *Palaeogeogr., Palaeoclimatol., Palaeoecol.* **273**, 302–328.

Huang J., Chu X., Lyons T. W., Planavsky N. J. and Wen H. (2013) A new look at saponite formation and its implications for early animal records in the Ediacaran of South China. *Geobiology* **11**, 3–14.

Huckriede H. and Meischner D. (1996) Origin and environment of manganese-rich sediments within black-shale basin. *Geochim. Cosmochim. Acta* **60**, 1399–1413.

Jiang G., Kaufman A. J., Christie-Blick N., Zhang S. and Wu H. (2007) Carbon isotope variability across the Ediacaran Yangtze platform in South China: implications for a large surface-to-deep ocean $\delta^{13}C$ gradient. *Earth Planet. Sci. Lett.* **261**, 303–320.

Jiang G., Shi X., Zhang S., Wang Y. and Xiao S. (2011) Stratigraphy and paleogeography of the Ediacaran Doushantuo Formation (ca. 635–551 Ma) in South China. *Gondwana Res.* **19**, 831–849.

Jin C., Li C., Algeo T. J., O'Connell B., Cheng M., Shi W., Shen J. and Planavsky N. J. (2018) Highly heterogeneous "poikiloredox" conditions in the early Ediacaran Yangtze Sea. *Precambrian Res.* **311**, 157–166.

Johnston D. T., Poulton S. W., Tosca N. J., O'Brien T., Halverson G. P., Schrag D. P. and Macdonald F. A. (2013) Searching for an oxygenation event in the fossiliferous Ediacaran of northwestern Canada. *Chem. Geol.* **362**, 273–286.

Kendall B., Komiya T., Lyons T. W., Bates S. M., Gordon G. W., Romaniello S. J., Jiang G., Creaser R. A., Xiao S., McFadden K., Sawaki Y., Tahata M., Shu D., Han J., Li Y., Chu X. and Anbar A. D. (2015) Uranium and molybdenum isotope evidence for an episode of widespread ocean oxygenation during the late Ediacaran Period. *Geochim. Cosmochim. Acta* **156**, 173–193.

Kendall B., Dahl T. W. and Anbar A. D. (2017) Good golly, why Moly? The stable isotope geochemistry of molybdenum. *Rev. Mineral. Geochem.* **82**, 682–732.

King E. K., Perakis S. S. and Pett-Ridge J. C. (2018) Molybdenum isotope fractionation during adsorption to organic matter. *Geochim. Cosmochim. Acta* **222**, 584–598.

Knoll A. H. (2011) The multiple origins of complex multicellularity. *Annu. Rev. Earth Planet. Sci.* **39**, 217–239.

Lenton T. M., Boyle R. A., Poulton S. W., Shields-Zhou G. A. and Butterfield N. J. (2014) Co-evolution of eukaryotes and ocean oxygenation in the Neoproterozoic era. *Nat. Geosci.* **7**, 257.

Lenz C., Jilbert T., Conley D. J., Wolthers M. and Slomp C. P. (2015) Are recent changes in sediment manganese sequestration in the euxinic basins of the Baltic Sea linked to the expansion of hypoxia? *Biogeosciences* **12**, 4875–4894.

Lowenstein T. K., Kendall B. and Anbar A. D. (2013) The geologic history of seawater. In Treatise on Geochemistry: Second Edition 8, 569–622. Elsevier Inc. https://doi.org/10.1016/B978-0-08-095975-7.00621-5.

McFadden K. A., Huang J., Chu X., Jiang G., Kaufman A. J., Zhou C., Yuan X. and Xiao S. (2008) Pulsed oxidation and biological evolution in the Ediacaran Doushantuo Formation. *Proc. Natl. Acad. Sci.* **105**, 3197–3202.

Meyer K. M. and Kump L. R. (2008) Oceanic euxinia in Earth history: causes and consequences. *Annu. Rev. Earth Planet. Sci.* **36**, 251–288.

Miller A. J., Strauss J. V., Halverson G. P., Macdonald F. A., Johnston D. T. and Sperling E. A. (2017) Tracking the onset of Phanerozoic-style redox-sensitive trace metal enrichments: new results from basal Ediacaran post-glacial strata in NW Canada. *Chem. Geol.* **457**, 24–37.

Miller C. A., Peucker-Ehrenbrink B., Walker B. D. and Marcantonio F. (2011) Re-assessing the surface cycling of molybdenum and rhenium. *Geochim. Cosmochim. Acta* **75**, 7146–7179.

Morford J. L. and Emerson E. (1999) The geochemistry of redox sensitive trace metals in sediments. *Geochim. Cosmochim. Acta* **63**, 1735–1750.

Morford J. L., Emerson S. R., Breckel E. J. and Kim S. H. (2005) Diagenesis of oxyanions (V, U, Re, and Mo) in pore waters and sediments from a continental margin. *Geochim. Cosmochim. Acta* **69**, 5021–5032.

Morris A. W. (1975) Dissolved molybdenum and vanadium in the northeast Atlantic Ocean. *Deep-Sea Research* **22**, 49–54.

Nägler T. F., Neubert N., Bottcher M. E., Dellwig O. and Schnetger B. (2011) Molybdenum isotope fractionation in pelagic euxinia: evidence from the modern Black and Baltic Seas. *Chem. Geol.* **289**, 1–11.

Nägler T. F., Anbar A. D., Archer C., Goldberg T., Gordon G. W., Greber N. D., Siebert C., Sohrin Y. and Vance D. (2014) Proposal for an international molybdenum isotope measurement standard and data representation. *Geostand. Geoanal. Res.* **38**, 149–151.

Nameroff T. J., Balistrieri L. S. and Murray J. W. (2002) Suboxic trace metal geochemistry in the eastern tropical North Pacific. *Geochim. Cosmochim. Acta* **66**, 1139–1158.

Neubert N., Nägler T. F. and Böttcher M. E. (2008) Sulfidity controls molybdenum isotope fractionation into euxinic sedi-

ments: evidence from the modern Black Sea. *Geology* **36**, 775–778.

Noordmann J., Weyer S., Montoya-Pino C., Dellwig O., Neubert N., Eckert S., Paetzel M. and Böttcher M. E. (2015) Uranium and molybdenum isotope systematics in modern euxinic basins: case studies from the central Baltic Sea and the Kyllaren fjord (Norway). *Chem. Geol.* **396**, 182–195.

Och L. M., Cremonese L., Shields-Zhou G. A., Poulton S. W., Struck U., Ling H., Li D., Chen X., Manning C. A., Thirlwall M., Strauss H. and Zhu M. (2016) Paleoceanographic controls on spatial redox distribution over the Yangtze Platform during the Ediacaran-Cambrian transition. *Sedimentology* **63**, 378–410.

Olson S. L., Ostrander C. M., Gregory D. D., Roy M., Anbar A. D. and Lyons T. W. (2019) Volcanically modulated pyrite burial and ocean-atmosphere oxidation. *Earth Planet. Sci. Lett.* **506**, 417–427.

Owens J. D., Lyons T. W., Li X., Macleod K. G., Gordon G., Kuypers M. M. M., Anbar A., Kuhnt W. and Severmann S. (2012) Iron isotope and trace metal records of iron cycling in the proto-North Atlantic during the Cenomanian-Turonian oceanic anoxic event (OAE-2). *Paleoceanography* **27**. https://doi.org/10.1029/2012PA002328.

Owens J. D., Gill B. C., Jenkyns H. C., Bates S. M., Severmann S., Kuypers M. M. M., Woodfine R. G. and Lyons T. W. (2013) Sulfur isotopes track the global extent and dynamics of euxinia during Cretaceous Oceanic Anoxic Event 2. *Proc. Natl. Acad. Sci.*, 18407–18412.

Owens J. D., Reinhard C. T., Rohrssen M., Love G. D. and Lyons T. W. (2016) Empirical links between trace metal cycling and marine microbial ecology during a large perturbation to Earth's carbon cycle. *Earth Planet. Sci. Lett.* **449**, 407–417.

Owens J. D., Lyons T. W. and Lowery C. M. (2018) Quantifying the missing sink for global organic carbon burial during a Cretaceous oceanic anoxic event. *Earth Planet. Sci. Lett.* **499**, 83–94.

Partin C. A., Bekker A., Planavsky N. J., Scott C. T., Gill B. C., Li C., Podkovyrov V., Maslov A., Konhauser K. O., Lalonde S. V., Love G. D., Poulton S. W. and Lyons T. W. (2013) Large-scale fluctuations in Precambrian atmospheric and oceanic oxygen levels from the record of U in shales. *Earth Planet. Sci. Lett.* **369–370**, 284–293.

Poulson R. L., Siebert C., McManus J. and Berelson W. M. (2006) Authigenic molybdenum isotope signatures in marine sediments. *Geology* **34**, 617–620.

Poulson Brucker R. L., McManus J., Severmann S. and Berelson W. M. (2009) Molybdenum behavior during early diagenesis: insights from Mo isotopes. *Geochem. Geophys. Geosyst.* **10**, Q06010.

Raiswell R., Hardisty D. S., Lyons T. W., Canfield D. E., Owens J. D., Planavsky N. J., Poulton S. W. and Reinhard C. T. (2018) The iron paleoredox proxies: a guide to pitfalls, problems and proper practice. *Am. J. Sci.* **318**, 491–526.

Reinhard C. T., Planavsky N. J., Robbins L. J., Partin C. A., Gill B. C., Lalonde S. V., Bekker A., Konhauser K. O. and Lyons T. W. (2013) Proterozoic ocean redox and biogeochemical stasis. *Proc. Natl. Acad. Sci.* **111**, 5357–5362.

Reinhard C. T., Planavsky N. J., Olson S. L. and Lyons T. W. (2016) Earth's oxygen cycle and the evolution of animal life. *Proc. Natl. Acad. Sci.* **113**, 8933–8938.

Rudnick R. L. and Gao S. (2003) Composition of the continental crust. In *The Crust*, vol. 3 (ed. R. L. Rudnick). Elsevier, pp. 1–64.

Sahoo S. K., Planavsky N. J., Kendall B., Wang X., Shi X., Scott C., Anbar A. D., Lyons T. W. and Jiang G. (2012) Ocean oxygenation in the wake of the Marinoan glaciation. *Nature* **489**, 546–549.

Sahoo S. K. (2015) Ediacaran ocean redox evolution. UNLV Theses. Dissertations, Professional Papers, and Capstones (Paper 2577).

Sahoo S. K., Planavsky N. J., Jiang G., Kendall B., Owens J. D., Wang X., Shi X., Anbar A. D. and Lyons T. W. (2016) Oceanic oxygenation events in the anoxic Ediacaran ocean. *Geobiology* **14**, 457–468.

Schneider A., Tanhua T., Roether W. and Steinfeldt R. (2014) Changes in ventilation of the Mediterranean Sea during the past 25 year. *Ocean Sci.* **10**, 1–16.

Scholz F., Hensen C., Noffke A., Rohde A., Liebetrau V. and Wallmann K. (2011) Early diagenesis of redox-sensitive trace metals in the Peru upwelling area – response to ENSO-related oxygen fluctuations in the water column. *Geochim. Cosmochim. Acta* **75**, 7257–7276.

Scholz F., McManus J. and Sommer S. (2013) The manganese and iron shuttle in a modern euxinic basin and implications for molybdenum cycling at euxinic ocean margins. *Chem. Geol.* **355**, 56–68.

Scholz F., Siebert C., Dale A. W. and Frank M. (2017) Intense molybdenum accumulation in sediments underneath a nitrogenous water column and implications for the reconstruction of paleo-redox conditions based on molybdenum isotopes. *Geochim. Cosmochim. Acta* **213**, 400–417.

Scholz F., Baum M., Siebert C., Eroglu S., Dale A. W., Naumann M. and Sommer S. (2018) Sedimentary molybdenum cycling in the aftermath of seawater inflow to the intermittently euxinic Gotland Deep, Central Baltic Sea. *Chem. Geol.* **491**, 27–38.

Scott C., Lyons T. W., Bekker A., Shen Y., Poulton S. W., Chu X. and Anbar A. D. (2008) Tracing the stepwise oxygenation of the Proterozoic ocean. *Nature* **452**, 456–459.

Scott C., Slack J. F. and Kelley K. D. (2017) The hyper-enrichment of V and Zn in black shales of the Late Devonian-Early Mississippian Bakken Formation (USA). *Chem. Geol.* **452**, 24–33.

Sheen A. I., Kendall B., Reinhard C. T., Creaser R. A., Lyons T. W., Bekker A., Poulton S. W. and Anbar A. D. (2018) A model for the oceanic mass balance of rhenium and implications for the extent of Proterozoic ocean anoxia. *Geochim. Cosmochim. Acta* **227**, 75–95.

Siebert C., Nägler T. F. and Kramers J. D. (2001) Determination of the molybdenum isotope fractionation by double-spike multi-collector inductively coupled plasma mass spectrometry. *Geochem., Geophys., Geosyst.* **2**, 2000GC000124.

Sperling E. A., Wolock C. J., Morgan A. S., Gill B. C., Kunzmann M., Halverson G. P., Macdonald F. A., Knoll A. H. and Johnston D. T. (2015) Statistical analysis of iron geochemical data suggests limited late Proterozoic oxygenation. *Nature* **523**, 451–454.

Tossell J. A. (2005) Calculating the partitioning of the isotopes of Mo between oxidic and sulfidic species in aqueous solution. *Geochim. Cosmochim. Acta* **69**, 2981–2993.

Tribovillard N., Algeo T. J., Lyons T. W. and Riboulleau A. (2006) Trace metals as paleoredox and paleoproductivity proxies: An update. *Chem. Geol.* **232**, 12–32.

Volkov I. I. (2000) Dissolved inorganic carbon and its isotopic composition in the waters of anoxic marine basin. *Oceanology* **40**, 499–502.

Wang L., Shi X. and Jiang G. (2012) Pyrite morphology and redox fluctuations recorded in the Ediacaran Doushantuo Formation. *Palaeogeogr., Palaeoclimatol., Palaeoecol.* **333**, 218–227.

Wang X., Jiang G., Shi X. and Xiao S. (2016) Paired carbonate and organic carbon isotope variations of the Ediacaran Doushantuo Formation from an upper slope section at Siduping, South China. *Precambrian Res.* **273**, 53–66.

Wasylenki L. E., Rolfe B. A., Weeks C. L., Spiro T. G. and Anbar A. D. (2008) Experimental investigation of the effects of temperature and ionic strength on Mo isotope fractionation during adsorption to manganese oxides. *Geochim. Cosmochim. Acta* **72**, 5997–6005.

Willbold M. and Elliot T. (2017) Molybdenum isotope variations in magmatic rocks. *Chem. Geol.* **449**, 253–268.

Associate editor: Silke Severmann